

Evaluating functional diversity indices as indicators of bird community responses to forest regeneration, northwest Ecuador

Nicole M. Lussier^{*1,2}, Jacob Woodlief¹, Colton B. Adams^{1,3}, Gregory Paladines², Jordan Karubian^{2,4}, J. Leighton Reid⁵, Charles Kwit^{1,6}

Corresponding Author*: nlussier@vols.utk.edu

1. Department of Ecology and Evolutionary Biology, University of Tennessee, Knoxville TN 37996, USA.
2. Fundación para la Conservación de Los Andes Tropicales, Quininde, Esmeraldas Province 080451, Ecuador.
3. Department of Psychology, University of Tennessee, Knoxville TN 37996, USA.
4. Department of Ecology and Evolutionary Biology, Tulane University, New Orleans LA, 70118, USA.
5. School of Plant and Environmental Sciences, Virginia Tech, Blacksburg, Virginia, USA
6. School of Natural Resources, University of Tennessee, Knoxville TN 37996, USA.

Acknowledgements: We would like to thank the staff and researchers at the Fundación para la Conservación de Los Andes Tropicales for their continued support and collaboration. We would also like to thank David Segurado, Miles Silman, Rakan Zahawi, and Holden Jones for allowing access to their drone imagery which was used in the data analysis of this work. Furthermore, we would like to thank the group of undergraduate researchers who aided in the data collection of this work, including Maggie Millar, John Huston, Erin Ortega, Lily Benson, Charlie Darmstadt, Taylor Mathes, and Courtney Velasquez, in addition to our field technicians and collaborators Rachel Crafford and Judith Santano. NML's data collection for this work was supported by the British Ecological Society (SR23\1280), the American Philanthropical Society, the American Ornithological Society, the Wilson Ornithological Society (Stewart23_NL), and the University of Tennessee. JLR was supported by the National Science Foundation (DEB 23-39839).

Author Contributions: Nicole Lussier conceived and planned the study. Nicole Lussier, Jacob Woodlief, Colton Adams, and Gregory Paladines collected and analyzed data. Jordan Karubian, J. Leighton Reid, and Charles Kwit were involved in planning, supervised the work, and aided in interpreting results and editing the manuscript. Nicole Lussier wrote the manuscript. All authors discussed results and commented on the manuscript.

Data Availability: The datasets generated during and/or analyzed during the current study are available from the corresponding author on reasonable request.

Declaration: The authors have no competing interests to declare that are relevant to the content of this article.

Evaluating functional diversity indices as indicators of bird community responses to forest regeneration, northwest Ecuador

Abstract

As biodiversity recovery remains a key component of conservation and restoration goals worldwide, conducting accurate community recovery assessments remains a significant challenge for restoration ecology. Community assessments have traditionally relied on taxonomic diversity indices; however, it has been recently suggested that functional diversity indices may provide informative measures of community recovery. Yet, the extent to which these metrics reliably predict community responses during forest regeneration remains uncertain. In this study, we tested the relationship between taxonomic and functional diversity indices in understory bird communities in relation to forest regeneration in the Chocó rainforest of northwest Ecuador. We sampled bird communities across varying forest regeneration classes and utilized LiDAR-derived canopy-level vegetation indices to examine relationships between diversity indices and developing forest structure. Unexpectedly, we observed an inverse relationship between most taxonomic and functional diversity measures as a function of forest regeneration. High species richness, diversity, and functional richness were associated with open-canopy habitats within the early stages of forest regeneration due to a high presence of generalist, disturbance-tolerant species. In contrast, high functional dispersion, functional divergence, and Rao's quadratic entropy were all associated with closed-canopy habitats and later stages of forest regeneration and were mainly driven by differences in beak and wing length. Therefore, not all functional diversity indices indicate the recovery of late-successional

understory bird communities. Unlike functional richness, measures such as functional dispersion, functional divergence, and Rao's quadratic entropy are weighted by species abundances and dominant traits within each community and better explain the shifts in composition between habitats. Thus, these measures could be more useful in assessing faunal community responses to forest regeneration. However, functional diversity measures were only indicative of changes between open and closed canopy habitats, where pairwise comparisons did not show differences between secondary and old-growth forest systems. Lastly, as the observed low levels of species richness in older forests were likely due to lower detection rates from mist-netting, higher levels of functional diversity within these habitats indicate that functional diversity can be assessed with less sampling, offering a more efficient approach to evaluating community responses to forest regeneration.

Keywords: Avian Communities, Chocó Biogeographic Zone, Ecological Restoration, Taxonomic Diversity, LiDAR Drone Imagery, Natural Regeneration

1 Introduction

2 Recognizing the regenerative capacity of tropical forests is crucial for addressing climate
3 change and biodiversity loss (Williams et al., 2024). Natural regeneration offers a large-scale,
4 cost-effective solution to forest loss, particularly in areas where forests can recover with minimal
5 human intervention (Bodin et al., 2022; Chazdon & Guariguata, 2016; Williams et al., 2024).
6 Biodiversity measurements of faunal communities within stages of natural regeneration are
7 typically used as indicators of restoration trajectories, as community dynamics can often give
8 insights into the functional recovery of tropical forests (Crouzeilles et al., 2016; Derhé et al.,
9 2018). This is typically done using taxonomic diversity indices (species richness and abundance),
10 which may fail to capture the full range of functional contributions within a community
11 (Acevedo-Charry & Aide, 2019; Crouzeilles et al., 2016; Moreno-Mateos et al., 2020). Thus,
12 functional diversity indices are becoming increasingly popular to evaluate community responses
13 to tropical forest regeneration, as they consider both species richness and abundance in
14 combination with traits relative to species ecological roles (Derhé et al., 2018; O'Brien et al.,
15 2022). However, the extent to which functional diversity indices reliably predict successional
16 patterns, and which measurements are reliably indicative of forest regeneration, are not well
17 understood. Therefore, this study aims to understand the drivers of functional diversity across
18 forest regeneration and to identify which diversity measures might be useful indicators for
19 restoration and conservation initiatives.

20 Tropical forest regeneration depends on the reassembly of functionally significant
21 species, such as tropical birds (Bello et al., 2024; Carlo & Morales, 2016; Lee, 2018). Many
22 studies have utilized bird communities as a tool to compare stages of forest regeneration and
23 restoration success (Barros et al., 2022; Helms et al., 2018; Latja et al., 2016). Birds play a

24 critical role in forest regeneration by dispersing seeds for the majority of tropical woody plants
25 (>85%), especially in degraded areas where seed availability limits recovery (Holl, 1999; Howe
26 & Smallwood, 1982; Wunderle, 1997). In addition, nectivorous and insectivorous birds influence
27 energy pathways critical to forest regrowth, as studies have shown that they consume up to 2.5
28 times more resources in open forests compared to old-growth systems (Malhi et al., 2022).
29 Insectivorous birds are important predators of herbivores, reducing leaf damage on regenerating
30 trees (Morrison & Lindell, 2012). Pollinators also facilitate gene flow of plants, which is
31 important for the long-term viability of plant populations (Kormann et al., 2016). Furthermore,
32 bird communities can rapidly recolonize disturbed areas depending on local environmental
33 conditions such as vegetation structure, resource availability, and remnant vegetation (Helms et
34 al., 2018; Latja et al., 2016; Reid et al., 2012).

35 Typically, bird communities transition over stages of forest regeneration to become more
36 similar to mature forest communities over time (Owen et al., 2020). However, the functional
37 recovery of bird communities is inconsistent. Some studies report an increase in functional
38 diversity in bird communities in areas with greater vegetation density and canopy structure
39 within early forest regeneration types (Coddington et al., 2023; Remeš et al., 2021), while others
40 have found no variation in functional diversity across stages and types of tropical forest
41 restoration (Barros et al., 2022). Furthermore, a recent study found that both functional diversity
42 and taxonomic diversity decreased as forest recovery progressed (Kortmann et al., 2025). These
43 discrepancies highlight the need to understand what functional diversity indices are useful
44 indicators of forest regeneration, and which might be less helpful in understanding community
45 shifts related to forest succession.

46 Regenerating vegetation plays a key role in shaping bird distribution and abundance
47 (Cano-Barbacid et al., 2023; Gregory & Gaston, 2000). Regenerating vegetation structure can be
48 assessed using LiDAR (Light Detection and Ranging) imagery. LiDAR imagery is emerging as a
49 transformative tool in restoration ecology, as its ability to capture three-dimensional data makes
50 it particularly valuable for assessing habitat structure and biodiversity within regenerating
51 ecosystems (Viana-Soto et al., 2022). LiDAR is growing particularly important for monitoring
52 structural components of forest regeneration such as vegetation density, complexity, and health
53 (Coops et al., 2021). Functional diversity measures have been shown to strongly associate with
54 vegetation indices (e.g., canopy height, vegetation density, leaf-area density) in tropical
55 secondary and old-growth forests (Coddington et al., 2023; Zahawi et al., 2015). In the initial
56 stages of forest succession, younger forests will have lower basal area, open canopies, and a lack
57 of tall trees (Finegan 1996; Aide et al., 2000). In later stages of succession, mature forests
58 typically consist of larger trees and denser canopies, with a range of vegetation heights and
59 features such as tree cavities, fostering higher species complexity (Remeš et al., 2021; Vesk et
60 al., 2008). The use of LiDAR technology to analyze forest regeneration could enhance our ability
61 to predict which elements of vegetation recovery are crucial for facilitating the recovery of
62 functional diverse animal communities.

63 In this study, we utilized a regenerating forest gradient and LiDAR-derived vegetation
64 indices to investigate their relationships between the composition, taxonomic diversity, and
65 functional diversity of understory avian communities in the Chocó rainforest of northwest
66 Ecuador. Specifically, we aimed to: (1) investigate the composition, taxonomic diversity, and
67 functional diversity of bird communities in relation to changes in forest regeneration, (2) test for
68 associations between diversity indices and vegetation structure, and (3) determine how functional

69 traits shift across stages of regeneration, and which traits and environmental variables contribute
70 most to changes in functional diversity. We hypothesized that avian community composition will
71 vary with forest regeneration, where differences in forest structure will act as a filter on avian
72 species composition. Furthermore, we hypothesized that both taxonomic and functional diversity
73 of avian communities will increase with forest regeneration and canopy-level attributes, as older,
74 structurally complex habitats provide a wider range of resources and niches. The increase in
75 avian functional diversity is expected to reflect a more specialized array of foraging behaviors
76 and habitat use in older regenerating forests. Through this research, we aim to a more
77 comprehensive understanding of what diversity indices might be most effective, efficient, and
78 applicable to conservation and restoration strategies as they relate to assessing community
79 responses to tropical forest regeneration.

80 **Methods**

81 **Study site**

82 This study was conducted at the Fundación para la Conservación de Los Andes
83 Tropicales (FCAT) Reserve within the greater Mache-Chindul Ecological Reserve (REMACH),
84 a key remnant patch of the Chocó rainforest in northwest Ecuador. The Chocó rainforest is a
85 globally recognized biodiversity hotspot with high levels of endemism (Aguilar Mugica et al.,
86 2009). REMACH encompasses 165,000 hectares (ha) of humid Chocó rainforest, wetlands, and
87 streams within the Rio Esmeraldas drainage, though it is affected by severe rates of deforestation
88 (Durães et al., 2013; Klemann et al., 2022; Van Der Hoek, 2017).

89 The FCAT Reserve covered 656 ha during the data collection period and ranged from
90 350–550 meters (m) above sea level (asl), with a wet season extending from January to June and
91 a dry season from July to December. The research design included 20 plots evenly distributed

92 across four habitat categories: highly impacted early successional habitat (HIE), low impact early
93 successional habitat (LIE), mid-successional secondary forest (SEC), and old growth Chocó
94 rainforest (OG) (Figure 1). HIE plots were cleared and used as cattle pastures for >20 years until
95 they were abandoned in 2021 when they were purchased by FCAT. LIE plots had lower levels of
96 disturbance, where selective logging and ≤ 1 year of grazing cattle from 2020–2021 without fire
97 or use of herbicides resulted in less soil compaction and more remnant trees and fruiting
98 vegetation (M Sanchez-Julia, *unpublished data*). SEC areas were predominantly abandoned
99 cocoa plantations that have been naturally regenerating for approximately 25 years. OG
100 represents old growth Chocó rainforest with limited recent human intervention (i.e., low intensity
101 selective logging) that surrounds all other plot categories. Sampling took place in five replicates
102 across each of the five regenerating forest types for a total of 20 plots spaced a minimum of 100
103 m apart throughout the FCAT Reserve.

104

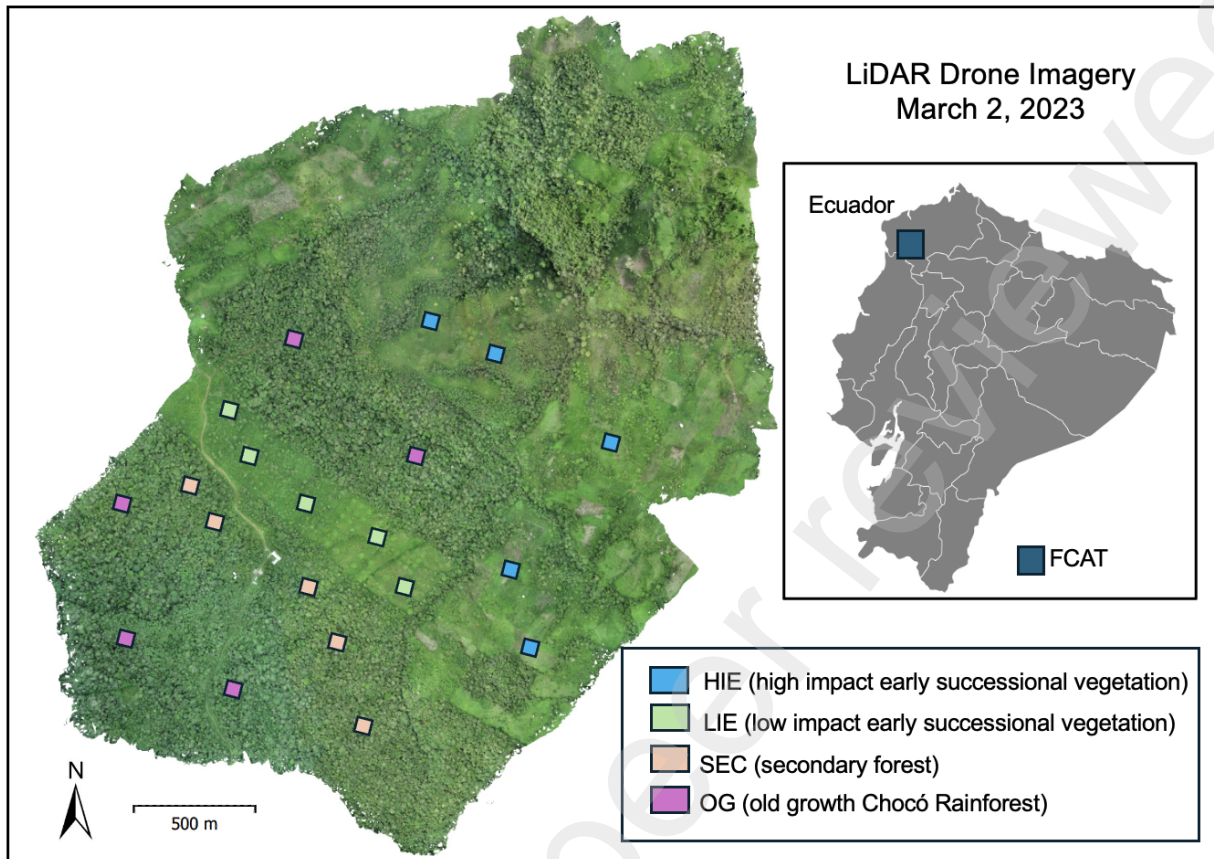


Figure 1: Sampling localities for avian communities within the FCAT Reserve. Sampling took place in 20 plots among four stages of forest regeneration: highly impacted early successional habitat (HIE, blue squares), low impact early successional habitat (LIE, green squares), mid-successional secondary forest (SEC, orange squares), and old growth Chocó rainforest (OG, purple squares).

105 **Sampling for bird communities and functional traits**

106 We conducted bird surveys from May–August in 2022 and 2023 to coincide with the dry
 107 season and to include resident species rather than migratory species. In each plot, we used mist-
 108 netting to account for abundances of understory bird species. This took place in fair weather
 109 from sunrise (~06:30) to 12:30 for two consecutive days at each plot, and then we rotated to a

110 randomized plot in a different regeneration type. In total, we completed 120 mist-netting hours
111 for each plot (10 nets [120 m per net line] × 6 hours × 2 days), for a total of 2,400 netting hours
112 across all sites. Nets were checked every 20 minutes. Each time a bird was netted, it was placed
113 in a holding bag and brought to a banding station. Individuals were held in bags for no more than
114 15 minutes. Each bird we captured received a uniquely numbered aluminum band and was
115 identified using *Birds of Ecuador* field guide (Freile & Restall, 2018) before being released at the
116 point of capture. Fieldwork was conducted with MAATE permission (*Ministerio del Ambiente,*
117 *Agua y Transición Ecológica*) under permit number: MAATE-ARSFC-2022-2589.

118 **Calculating functional diversity indices**

119 To obtain functional traits for each species, we used an open-access dataset that contained
120 morphological, geographical, and behavioral traits for over 12,000 individual species (Tobias et
121 al., 2022). From this data set, we extracted both morphological (beak length (mm), beak width
122 (mm), wing length (mm), mass (g)) and behavioral (primary habitat, trophic niche) functional
123 traits for each observed species (Supplementary Table 1). These traits are relevant to forest
124 regeneration as they influence species foraging strategies, habitat usage, and dispersal abilities.
125 For example, changes in beak morphology may reflect adaptations to specific food resources
126 such as fruiting plant species, and changes in wing morphology may reflect species abilities to
127 maneuver between complex forest vegetation. Categorical traits were numerically coded (e.g.,
128 frugivore = 0, granivore = 1). To calculate functional diversity, we took the log transformation of
129 each continuous trait (beak length, wing length, tail length, mass) to normalize the data. We
130 excluded categorical traits (trophic niche, vertical habitat preference, disturbance-tolerance) from
131 functional diversity indices because the inclusion of categorical variables has been shown to
132 reduce the quality of the functional space (Maire et al., 2015).

133 The resultant trait matrix was paired with weighted abundance data for each regeneration
134 type, where each mist-netting plot was classified as a community. Then, we used the “*dbFD*”
135 function in the *FD* package in R to calculate functional diversity indices (Laliberté et al., 2014).
136 The FD index approach was used, which is the total branch lengths of a functional dendrogram
137 calculated with the Gower distance measure (Podani, 1999). This approach uses a species-trait
138 matrix, which is converted to a distance matrix (Gower distance), and then converted to a
139 dendrogram via the Unweighted Pair Group Method with Arithmetic Mean (UPGMA) clustering
140 method. We calculated functional evenness (FEve) and divergence (FDiv) using the convex hull
141 methodology (Villéger et al., 2008), which uses the Gower distance matrix with PCoA analysis
142 to calculate a matrix of transformed coordinates and then uses the PCoA matrices to calculate the
143 functional metrics. High FDiv means species abundances are concentrated towards the extremes
144 of the functional trait space, indicating a high degree of niche differentiation (Sayer et al., 2017).
145 This can occur in communities where a few species have very distinct functional traits that are
146 well-separated from each other. Finally, we calculated functional richness (FRic), Rao’s
147 Quadratic Entropy (Rao’s Q) and functional dispersion (FDis) using the methodology of Villéger
148 et al. 2008. FRic is the total range or variety of functional traits present among species within a
149 given area or habitat. Rao’s Q is a measure of functional diversity that considers both species
150 abundances and their pairwise functional dissimilarities. High Rao's Q indicates high
151 dissimilarity among species, even if the number of species and the total range of functional traits
152 (FRic) are low. FDis quantifies the variability or spread of species trait values within a
153 community where higher FDis indicates greater variability in traits among species, suggesting a
154 community with a wider range of ecological strategies.

155 **Calculating LiDAR-derived vegetation indices**

156 We calculated vegetation indices from LiDAR data captured by drone (EP800, 8.8mm,
157 resolution: 5472 x 3648 pixels) within the FCAT reserve on March 2, 2023. The process
158 involved initial data preprocessing to generate a high-resolution digital elevation model (DEM)
159 from the LiDAR point cloud data (Segurado & Silman, 2023). We utilized QGIS for
160 segmentation and classification techniques to delineate canopy features and estimate height and
161 elevation. Elevation for each point was calculated using the DEM. Elevation among our sites
162 ranged from 416–656 m-asl. To calculate canopy height, the LiDAR data were processed to
163 generate a Digital Surface Model (DSM) and Digital Terrain Model (DTM), and the canopy
164 height was calculated by subtracting the DTM from the DSM using the raster calculator in QGIS.
165 Canopy openness, indicative of light penetration through the canopy, was derived by evaluating
166 gaps in vegetation cover. We calculated canopy openness by setting a threshold value (15 m
167 from ground) to classify pixels based on their height allowing for the determination of open areas
168 within the canopy. The resulting raster layer displayed the percentage of openness across the
169 landscape. Canopy cover, representing the extent of foliage within an area, is quantified by
170 assessing the area occupied by the canopy in relation to the total area. For the canopy cover
171 assessment, we manually classified LiDAR points corresponding to vegetation at a minimum of
172 15 m from ground level, and the ratio of classified vegetation points to the total area. Finally, we
173 used the density tool to assess distances between canopy points and compute canopy gaps, which
174 allowed us to obtain measures of canopy cover for each plot. We then tested multicollinearity
175 between environmental variables using Spearman's correlation from the *stats* package (Dormann
176 et al., 2013). We found evidence of collinearity between canopy height and canopy openness (S
177 = 1932, $p = 0.047$), thus we removed canopy openness from models. Therefore, environmental
178 variables included canopy height, canopy cover, and elevation.

179 **Statistical analyses**

180 All statistical analyses and models were fitted in R (R Core Team, 2022). Abundance
181 data from mist-netting were compiled together into a weighted matrix, where rows represented
182 mist-netting plots (five individual communities per regeneration type), and columns represented
183 individual bird species. Birds observed within mist-netting trials were weighted by their
184 abundance due to our ability to identify individuals from aluminum bands, which allowed us to
185 avoid counting the same individual twice. The resultant weighted adjacency matrix was then
186 used to assess differences in bird communities and taxonomic and functional diversity metrics
187 across each regeneration type. We used these data to calculate Hill numbers using the *iNEXT*
188 package in R (Chao et al., 2014): $q = 0$ (species richness), Hill $q = 1$ (exponential of Shannon's
189 diversity index), and Hill $q = 2$ (inverse of Simpson's index) (Ellison, 2010). Rarefaction and
190 extrapolated curves were generated to determine how taxonomic diversity increases with
191 increasing sampling effort and completeness. Rarefaction and extrapolation of richness, Shannon
192 diversity, and Simpson diversity were calculated for each mist-netting plot (Chao et al., 2014).
193 Sample-based curves evaluated the number of individuals in a sample by plotting diversity
194 estimates in relation to the number of sampling units, while coverage-based curves were plotted
195 against rarefied completeness in relation to sample coverage. Curves were plotted using doubling
196 of sampling size, and 999 bootstrap replicates were used to estimate 95% confidence intervals.

197 To test for differences in the composition of understory bird communities across the
198 regeneration gradient, we used abundance data from the adjacency matrix to calculate
199 dissimilarity between plots using the Bray-Curtis dissimilarity index and the “*vegdist*” function
200 in the *vegan* package in R (Oksanen et al., 2022). The Bray-Curtis index accounts for differences
201 in species composition and abundance between plots, providing a measure of dissimilarity that

202 ranges from 0 (identical communities) to 1 (completely different communities with no
203 overlapping species). To evaluate statistical support for differences in avian communities across
204 regenerating stages, we performed a Permutational Multivariate Analysis of Variance
205 (permanova) using the “*adonis*” function in the *vegan* package. Then, to assess the relationship
206 between bird community composition and environmental variables, we used a Redundancy
207 Analysis (RDA). First, the abundance matrix was normalized using the Hellinger transformation
208 (Legendre & Gallagher, 2001). We plotted the RDA using the “*rda*” function in the *vegan*
209 package in R and fitted relative environmental variables to the model using the “*anova.cca*”
210 function with 1000 null model iterations. To determine if specific trophic niches (e.g.,
211 frugivores) within communities differed across regeneration types, we used categorical data to
212 perform a chi-squared test using the “*chisq.test*” function in the *stats* package in R.

213 When considering differences in taxonomic and functional diversity indices, we first
214 tested for spatial autocorrelation using the *spdep* package in R. We created a distance matrix
215 from the UTM Northing and Easting coordinates of each sampling location. Next, we used the
216 *spdep* package to construct a neighborhood structure based on this distance matrix, converting
217 the neighbor list into spatial weights. This allowed us to assess spatial autocorrelation through
218 Moran’s I test. We found evidence of spatial autocorrelation for several of our response
219 variables. Therefore, we performed Generalized Least Squares (GLS) analyses incorporating a
220 Gaussian correlation structure. We chose Gaussian correlations because they allow for a
221 continuous decay of spatial autocorrelation over distance, which is more appropriate for
222 modeling the gradual environmental gradients and the spatial structure in our dataset compared
223 to alternative correlation structures that may assume more abrupt changes. The Gaussian
224 correlation structure was defined using plot coordinates (easting and northing).

225 For diversity metrics that exhibited significant spatial autocorrelation, we applied GLS
226 regression to account for spatial dependence in model residuals. To evaluate differences in
227 taxonomic and functional diversity across sites, we then modeled taxonomic and functional
228 diversity metrics first as functions of regeneration type, then as functions of environmental
229 variables. Both sets of models retained the Gaussian spatial correlation structure to account for
230 spatial dependence. We used Type II Wald chi-square tests for response variables as a function
231 of regeneration type. We used Type III tests for response variables as a function of
232 environmental variables due to the interaction between canopy cover and canopy height, which
233 was included in models. We then plotted all relationships using the *ggplot2* package (Wickham
234 et al., 2016).

235 Finally, to determine how functional traits shift across stages of regeneration, and which
236 traits contribute most to changes in functional diversity, we ran a redundancy analysis (RDA)
237 between species abundances across regeneration types, with functional traits as explanatory
238 variables. We tested the significance of each explanatory variable using ANOVA-like
239 permutation tests under the “*anova.cca*” function with 1,000 permutations applied to evaluate
240 individual variable contributions. The “*envfit*” function was again used to fit explanatory
241 variables onto the RDA ordination, and p-values were extracted to determine which variables
242 significantly influenced community structure. Variables with $p < 0.05$ were classified as
243 significant. To examine correlations among explanatory variables, a Pearson correlation matrix
244 was computed using the “*cor*” function in the *vegan* package for each diversity measure and
245 functional trait.

246 **Results**

247 **Avian community composition differed as a function of forest regeneration**

248 We recorded a total of 940 individual birds representing 111 different species across all
249 study sites (Supplementary Table 1). Among these, the most frequently observed species were
250 *Phaethornis yaruqui* (White-whiskered Hermit, $n = 98$), *Asemospiza obscura* (Dull-colored
251 Grassquit, $n = 64$), and *Sporophila funerea* (Thick-billed Seed Finch, $n = 48$). Rarefaction
252 analysis showed that our sampling effort captured 83–90% of total species richness, 89% of
253 species diversity, and 95% of community evenness (Supplementary Figure 1). Understory bird
254 communities differed as a function of regeneration type ($r^2 = 0.47$, $F = 4.68$, $p \leq 0.01$) (Figure 2).
255 Species richness also varied among regeneration type ($r^2 = 0.64$, $F = 12.40$, $p \leq 0.01$), where low-
256 impacted plots (LIE) had the highest species richness observed (mean = 27.6, variance = 7.8),
257 followed by high-impact early successional (HIE) plots (mean = 25.4, variance = 41.3).
258 Furthermore, bird abundances varied significantly across sites ($r^2 = 0.43$, $F = 5.70$, $p \leq 0.01$),
259 where the highest bird abundances were recorded in HIE (mean = 56.8, variance = 796) and LIE
260 plots (mean = 66.6, variance = 134.3), while SEC and OG plots had comparatively lower bird
261 numbers (SEC: mean = 37.8, variance = 123.7; OG: mean = 26.8, variance = 83.7).

262 Both canopy cover and canopy height were higher in older forests (SEC and OG) than in
263 younger sites (HIE and LIE) (cover: $r^2 = 0.83$, $p \leq 0.01$, height: $r^2 = 0.83$, $p \leq 0.01$) (Table 1).
264 Elevation was also different across regenerating stages, where younger sites (HIE and LIE) were
265 lower in elevation than older sites (SEC and OG) ($r^2 = 0.63$, $p \leq 0.01$). Considering communities
266 of understory birds across regeneration types, canopy height was the biggest predictor of
267 community differences in terms of environmental variables (variance = 0.16, $F = 5.82$, $p \leq 0.01$).
268 Canopy height demonstrated strong associations with RDA 1 (0.98), whereas canopy cover

269 exhibited a weaker and non-significant positive relationship with RDA 1 (0.98) and RDA 2
270 (0.05) (variance = 0.02, $F = 0.92$, $p = 0.47$). Elevation also had a non-significant relationship
271 (variance = 0.03, $F = 0.98$, $p = 0.36$) with RDA 1 (0.53) and RDA 2 (-0.85) suggesting a lesser
272 influence on the observed variation in the dataset. Constrained variables explained about 35.4%
273 of the total variance in our RDA.

274 **Taxonomic and functional diversity differed across forest regeneration stages**

275 Both taxonomic and functional diversity of understory bird communities differed as a
276 function of regeneration stage (Supplementary Table 3). Expected species richness (Q_0) and
277 species diversity (Q_1) were highest in high-impact early successional sites and declined in mature
278 forests (Figure 3). In contrast, when minimizing the influence rarer species using Inverse
279 Simpson Index (Q_2), we observed that older forests (SEC and OG) had higher diversity than
280 younger successional sites. While changes in species richness (Q_0) and the Inverse Simpson
281 Index (Q_2) were not associated with any environmental predictor, Shannon entropy (Q_1) was
282 driven by changes in canopy height and decreased with increasing canopy (chi-squared = 4.92, p
283 = 0.03) (Table 3). Functional diversity indices exhibited a similar trend as Q_2 ; functional
284 dispersion, functional divergence, and RaoQ were all greater in mature forests (SEC and OG)
285 than in early successional ones (HIE and LIE) (Figure 3). Pairwise tests showed that functional
286 divergence of bird communities differed between high impact sites and secondary forests ($p =$
287 0.05), high impact sites and old growth forests ($p = 0.02$), and low-impact sites and old growth
288 forests ($p = 0.03$). Functional divergence was strongly influenced by both canopy height (chi-
289 squared = 11.46, $p < 0.001$) and the interaction between canopy cover and height (chi-squared =
290 12.53, $p < 0.001$) (Table 2). Functional dispersion followed similar patterns and was higher in
291 later successional forests, with differences between early successional stages (HIE) and both

292 intermediate and mature forests (SEC, $p = 0.008$; OG, $p = 0.002$), and between LIE and later
293 stages (SEC, $p = 0.007$; OG, $p = 0.002$). Functional dispersion was also associated with both
294 canopy height (chi-squared = 5.63, $p = 0.02$), and the interaction between canopy cover and
295 height (chi-squared = 5.64, $p = 0.02$). Rao's Quadratic Entropy also varied between highly
296 impacted sites and old growth forests ($p = 0.02$), and low impacted sites with both secondary
297 forests ($p = 0.04$), and old growth forests ($p = 0.01$). Like dispersion and divergence, Rao's
298 Quadratic Entropy was also associated with both canopy height (chi-squared = 6.19, $p = 0.01$)
299 and the interaction between canopy cover and height (chi-squared = 6.87, $p = 0.01$). In contrast,
300 the functional richness of understory bird communities was lowest in the more mature forests
301 and highest in early successional areas ($p = 0.03$), and pairwise comparisons revealed that
302 functional richness only differed between early successional stages (HIE) and mature forests
303 (OG) ($p = 0.03$). Both functional richness and functional evenness were not driven by any
304 environmental predictor variables.

305 Both younger sites (HIE and LIE) clustered together on the RDA, indicating greater
306 functional similarity compared to mature forest plots (SEC and OG) (Figure 4). The RDA model
307 explained 64.73% of total variation in functional diversity (constrained inertia = 0.4122).
308 Functional richness was associated with open-canopy habitats (HIE and LIE), mainly driven by
309 variations in beak width and tarsus length. Both beak width and tarsus length were positively
310 associated with functional richness, yet were negatively associated with functional dispersion,
311 functional divergence, and Rao's Q (Figure 5). Functional dispersion, functional divergence,
312 Rao's Quadratic Entropy, and functional evenness were all indicators of closed canopy habitats
313 and associated with both SEC and OG. OG and SEC forests clustered together on the RDA but
314 exhibited distinct trait shifts. Specifically, changes in tail length, mass, and wing length were

315 associated with old growth forests, whereas changes in beak length were more strongly
316 associated to both OG and SEC habitats. Beak length was strongly correlated with differences in
317 functional dispersion (0.85), functional divergence (0.79), and Rao's Q (0.81), whereas wing
318 length was positively correlated with functional dispersion (0.55) and Rao's Q (0.67).
319

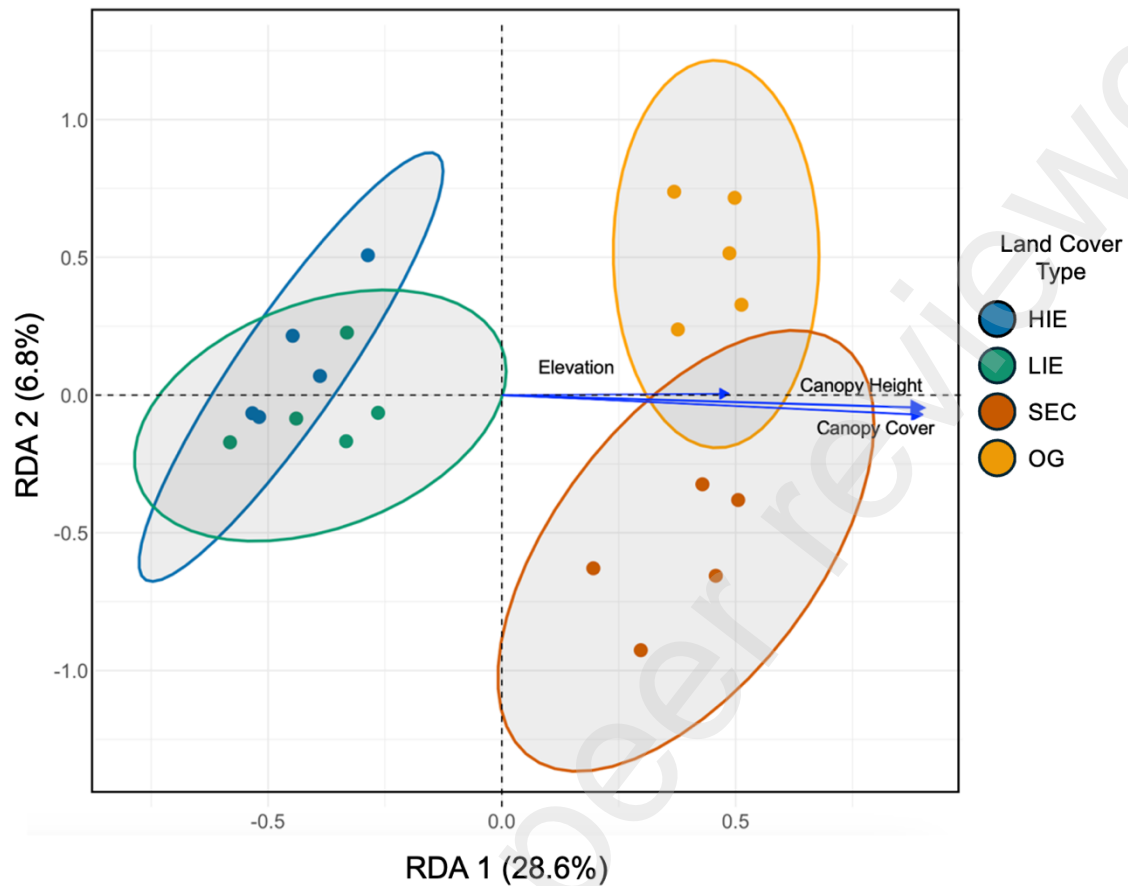


Figure 2: Redundancy Analysis (RDA) biplot of bird community composition constrained by selected environmental variables (canopy cover, canopy height, and elevation), and grouped by regeneration type (highly impacted early successional habitat (HIE, blue), low impact early successional habitat (LIE, green), mid-successional secondary forest (SEC, orange), and old growth Chocó rainforest (OG, yellow)). Points in the plot represent communities or individual plots and blue arrows represent environmental variables. The x-axis (RDA1) explains 28.6% of the variation in bird community composition. The y-axis (RDA2) explains 6.8% of the variation. The direction and length of the arrows indicate the strength and direction of the relationship between each environmental variable and the ordination axes. Samples located in the same direction as an arrow are positively associated with that environmental variable.

Table 1: Vegetation indices calculated from LiDAR data captured by drone within the FCAT Reserve.

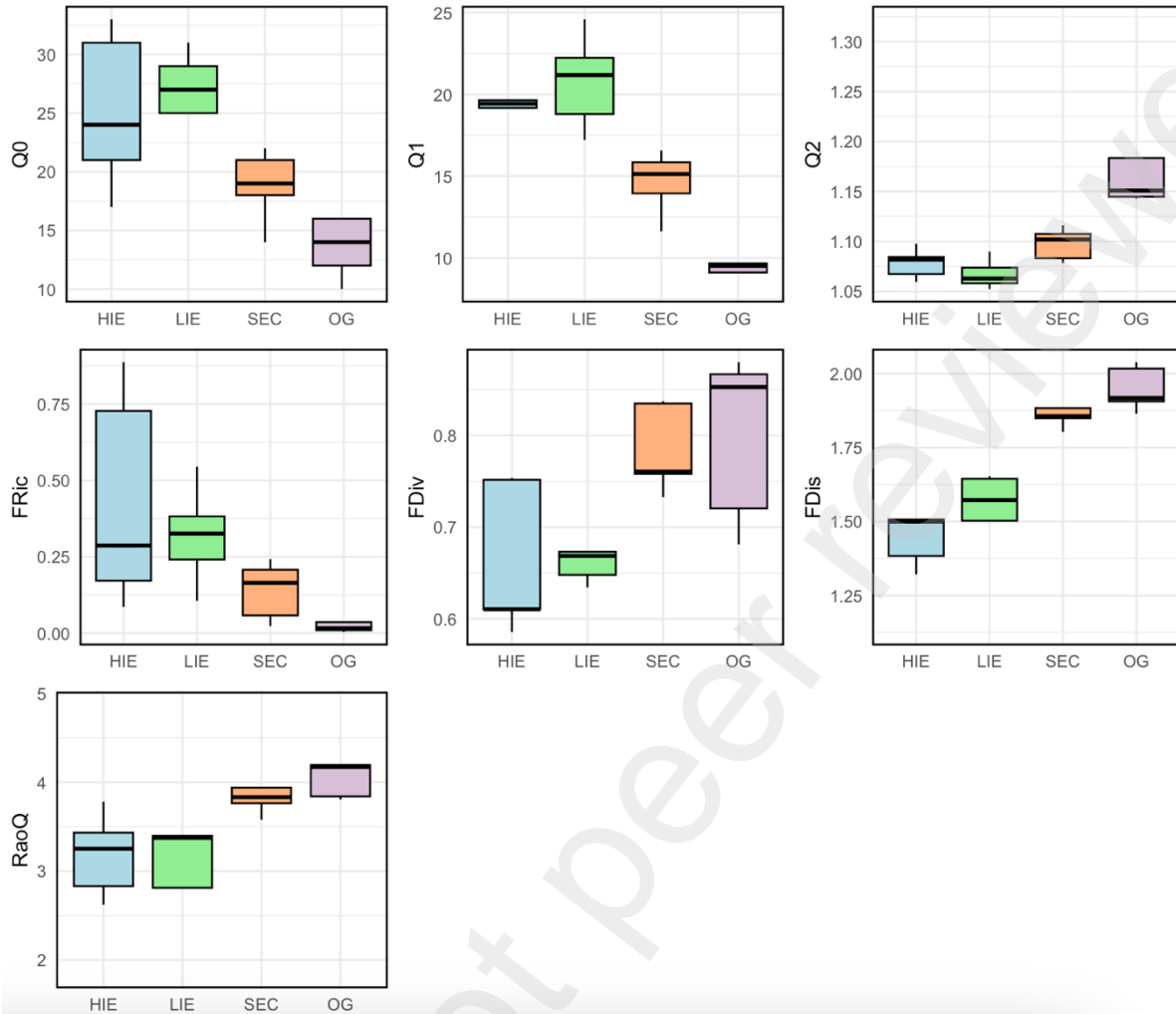
This included canopy height (m), canopy cover (%), canopy openness (%), and elevation (m-asl).

“Stage” represents the four regenerating forest categories: highly impacted early successional habitat (HIE), low impact early successional habitat (LIE), mid-successional secondary forest (SEC), and old growth Chocó rainforest (OG).

Regeneration Type	Value	Canopy Height (m)	Canopy Cover (%)	Canopy Openness (%)	Elevation (m-asl)
HIE	Mean	6.84 (± 3.11)	7.59 (± 4.56)	12.22 (± 1.04)	466.76 (± 1876.79)
LIE	Mean	4.93 (± 0.33)	11.31 (± 18.87)	14.12 (± 0.11)	539.94 (± 157.50)
SEC	Mean	27.22 (± 13.76)	26.42 (± 14.41)	12.86 (± 0.23)	533.54 (± 432.5)
OG	Mean	26.76 (± 94.98)	25.53 (± 33.07)	12.89 (± 0.11)	533.76 (± 140.65)

Table 2: Type III Wald chi-square tests assessing the effects of canopy cover, canopy height, elevation, and their interaction on taxonomic and functional diversity metrics. Generalized least squares (GLS) regression was used to account for spatial dependence in model residuals, with a Gaussian spatial correlation structure applied. Relationships are highlighted by + or – symbols, where + indicates a positive correlation between variables, and a – indicates a negative correlation between variables. Significant relationships ($p < 0.05$) are highlighted in bold with an asterisk (*).

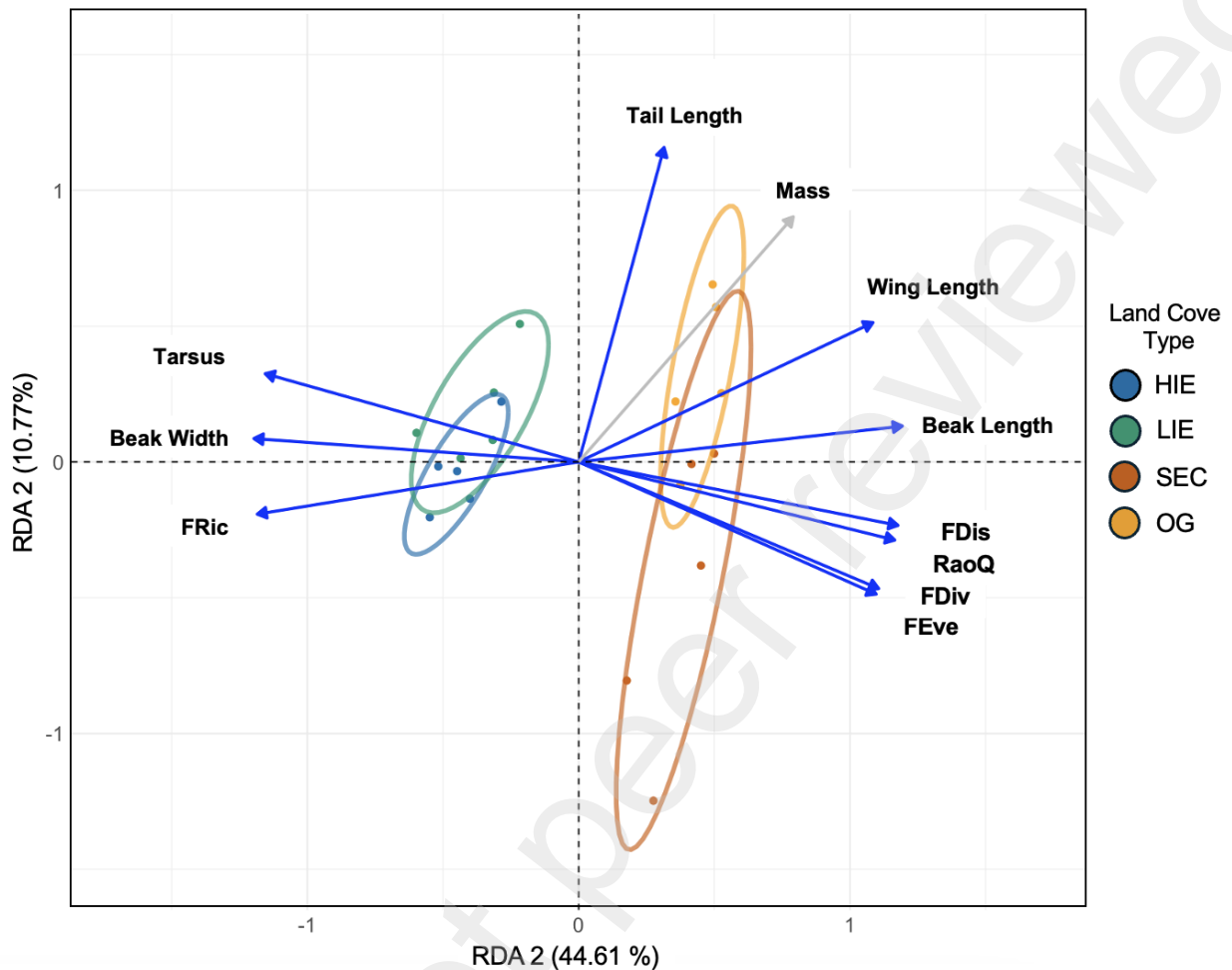
Response Variable	Predictor	Relation (+ or -)	Chi Squared	P-value
Species Richness (Q_0)	Canopy Cover	-	0.20	0.66
	Canopy Height	-	1.48	0.22
	Elevation	-	1.33	0.25
	Canopy Cover * Canopy Height	-	0.25	0.62
Shannon Entropy (Q_1)	Canopy Cover	-	0.06	0.81
	Canopy Height	-	4.92	0.03*
	Elevation	-	0.76	0.38
	Canopy Cover * Canopy Height	-	1.96	0.16
Inverse Simpson Index (Q_2)	Canopy Cover	+	0.07	0.79
	Canopy Height	+	4.36	0.04
	Elevation	+	0.38	0.54
	Canopy Cover * Canopy Height	+	2.41	0.12
Functional Richness (FRic)	Canopy Cover	-	0.00	0.98
	Canopy Height	-	0.05	0.82
	Elevation	-	1.72	0.19
	Canopy Cover * Canopy Height	-	0.01	0.93
Functional Divergence (FDiv)	Canopy Cover	+	1.18	0.28
	Canopy Height	+	11.46	< 0.001 *
	Elevation	+	3.28	0.07
	Canopy Cover * Canopy Height	+	12.53	< 0.001 *
Functional Evenness (FEve)	Canopy Cover	+	0.56	0.45
	Canopy Height	+	2.22	0.14
	Elevation	+	1.07	0.30
	Canopy Cover * Canopy Height	+	2.64	0.10
Functional Dispersion (FDis)	Canopy Cover	+	2.06	0.15
	Canopy Height	+	5.63	0.02 *
	Elevation	+	0.50	0.48
	Canopy Cover * Canopy Height	+	5.64	0.02 *
Rao's Quadratic Entropy (RaoQ)	Canopy Cover	+	2.67	0.10
	Canopy Height	+	6.19	0.01 *
	Elevation	+	0.47	0.49
	Canopy Cover * Canopy Height	+	6.87	0.01 *



324

325 **Figure 3:** Differences in Hill numbers (Q_0 = species richness, Q_1 = exponential of Shannon Entropy, Q_2 =
 326 Inverse Simpson Index) and functional diversity metrics (FDiv = functional divergence, FDis = functional
 327 dispersion, FRic = functional richness, RaoQ = Rao's Quadratic Entropy) across a regenerating forest
 328 gradient. Plots include highly impacted early successional habitat (HIE, blue), low impact early
 329 successional habitat (LIE, green), mid-successional secondary forest (SEC, orange), and old growth
 330 Chocó rainforest (OG, purple).

331



332

Figure 4: Redundancy Analysis (RDA) biplot illustrating the relationships between functional diversity indices, morphological traits, and community composition. Individual sample plots are represented by points corresponding to their regeneration type (HIE = blue, LIE = green, SEC = red, and OG = yellow). Arrows represent exploratory vectors, with blue arrows indicating variables that significantly ($p < 0.05$) explain variation in community composition, and gray arrows representing non-significant predictors. The x-axis (RDA1) explains 44.61% of the constrained variation, while the y-axis (RDA2) explains 10.77%. Functional diversity indices (FDis: Functional Dispersion, FDiv: Functional Divergence, FRic: Functional Richness, RaoQ: Rao's Quadratic Entropy) and

morphological traits were used as explanatory variables. Sites and species positioned closer together share more similar trait compositions. The direction and length of arrows indicate the strength and influence of each predictor on community structure.

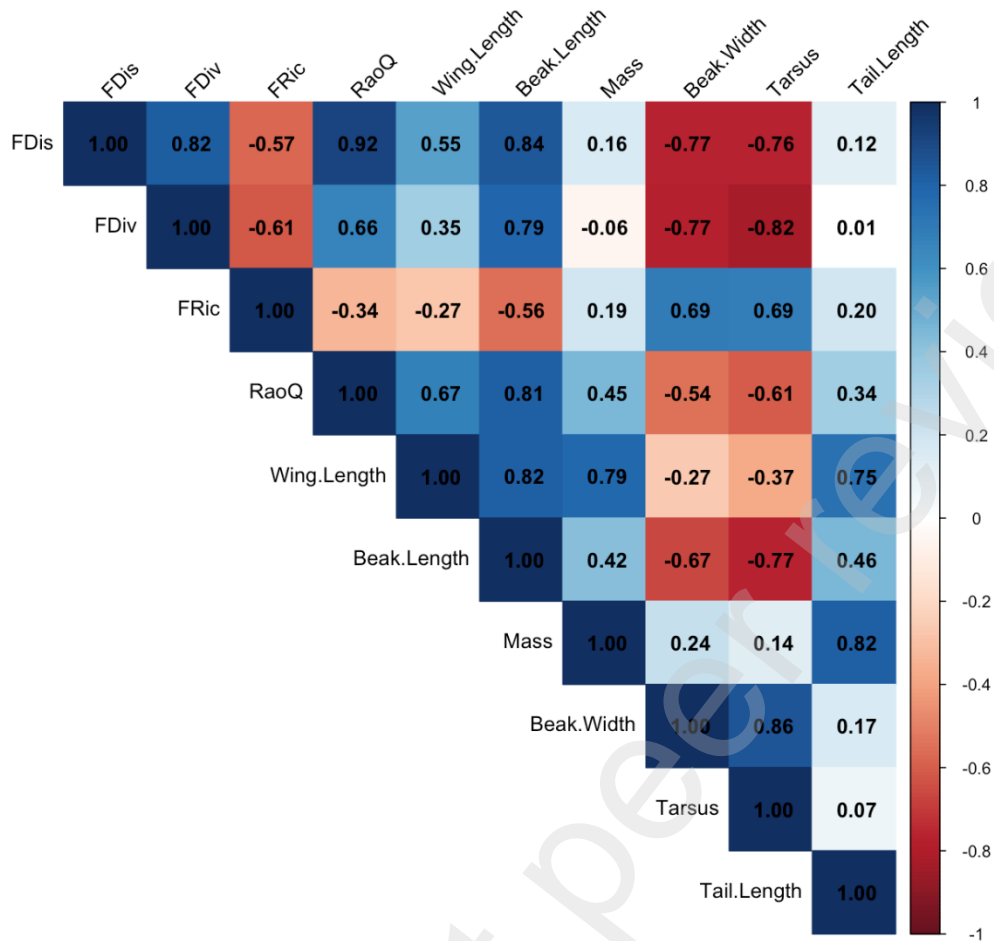


Figure 5: Pearson correlation matrix illustrating the relationships between functional diversity indices (FDis: Functional Dispersion, FDiv: Functional Divergence, FRic: Functional Richness, RaoQ: Rao's Quadratic Entropy) and morphological traits (Wing Length, Beak Length, Mass, Beak Width, Tarsus, Tail Length). The color intensity and shading represent the strength and direction of the correlations, with warmer colors (red) indicating strong positive correlations and cooler colors (blue) representing strong negative correlations. Correlation coefficients are displayed within the matrix, with significant relationships highlighted.

334 **Discussion**

335 The degree to which natural regeneration promotes functional and resilient communities is a
336 key question for ecological and conservation research. To address this question, expanding
337 diversity assessments, which have traditionally been taxonomically based, to incorporate
338 functional diversity indices will be an important step forward for understanding forest
339 regeneration as well as the field of conservation and restoration ecology (Chazdon, 2008, 2013;
340 Lamb, 2018; Nabhan et al., 2020). However, we found that different functional or taxonomic
341 diversity indices provided drastically different results, and that not all measures were equally
342 good indicators of forest regeneration. The strongest differences in bird functional and
343 taxonomic composition were between open and closed canopy environments, where most
344 taxonomic indices were highest in open canopy environments and most functional diversity
345 measures were highest in closed canopy environments. Functional richness was associated with
346 open-canopy habitats in early stages of regeneration, and functional evenness showed no changes
347 between regeneration stages. Inversely, functional divergence, functional dispersion, and Rao's
348 quadratic entropy increased as a function of canopy cover and height and were indicative of
349 forest communities. Therefore, functional divergence, functional dispersion, and Rao's quadratic
350 entropy might be more valuable to consider in community assessments within tropical forest
351 restoration.

352 The strongest differences in bird functional and taxonomic composition were associated with
353 vegetation changes between open and closed canopy environments. Functional dispersion,
354 functional divergence, and Rao's Q increased with canopy height and density independently of
355 bird species richness, indicating as forests grow taller and more structurally complex, the species
356 that persist have more distinct ecological roles (Remeš et al., 2021). This result is not surprising,

357 as functional diversity measures reflect deeper ecological processes that take longer to recover
358 compared to simpler metrics like species richness and abundance (Acevedo-Charry & Aide,
359 2019). Resources provided by taller vegetation might allow the coexistence of species with
360 diverse ecological strategies by providing more niche space (Aguirre-Gutiérrez et al., 2017;
361 Oliveira & Scheffers, 2019). Other work has found similar trends, where increased tree cover
362 positively correlated with increased guild richness and a greater distribution of functional traits
363 (Ikin et al., 2019). However, canopy attributes only explained 35% of the variance in bird
364 communities. Thus, other variables are important to consider, as factors such as food availability
365 can also influence functional diversity by filtering trait assemblages (Flynn et al., 2011; Pena et
366 al., 2023; Quitian et al., 2019). For instance, in a Peruvian cloud forest, early regeneration
367 habitats with dense understories supported more bird species with plant-based diets (flowers,
368 fruits, and seeds), broader elevational ranges, and wider habitat breadths compared to old-growth
369 forests (Ausprey et al., 2022). Furthermore, dispersal ability and historical contingency also
370 contribute to changes in community assembly (Gao et al., 2024), therefore could also contribute
371 to changes in functional diversity.

372 Species richness and Shannon's entropy were highest in early stages of forest regeneration,
373 likely due to the high abundance of generalist disturbance-tolerant species. Generalist species
374 adapted to fast population growth in resource-rich environments dominate earlier successional
375 stages, while species with higher competitive ability in resource-limited environments, or those
376 that depend on resources such as higher structural vegetation complexity, dominate older-growth
377 forests (Pinotti et al., 2012). However, functional richness was also associated with open-canopy
378 habitats, in contrast to functional dispersion, functional divergence, and Rao's quadratic
379 entropy). Functional richness is simply defined as the proportion of the total number of traits

380 available that are occupied by at least one individual, and may correlate with species richness
381 (Villéger et al., 2008). Therefore, functional richness is independent of species abundances
382 (Karadimou et al., 2016), and similar to species richness, will increase as the number of species
383 present increases regardless of species rarity. Thus, high species richness in early successional
384 plots could result in a wider range of functional traits present within a community, but not
385 necessarily equate to a more functionally diverse community overall. Differences in functional
386 richness across regeneration stages was explained by changes in beak width and tarsus length. In
387 this system, open canopy habitats were dominated by a high diversity of small, wide beaked
388 granivorous species including *Oryzoborus funereus*, *Sporophila corvina*, and *Sporophila*
389 *nigricollis*. Therefore, early successional habitats likely maintain a mix of open-area specialists
390 (e.g., ground-foraging species) and habitat-edge opportunists, but lack the ecological
391 specialization seen in forests (Ausprey et al., 2022). Thus, functional richness may not be a good
392 indicator of forest regeneration, similar to species richness, as it could lead to a biased
393 interpretation of recovery if the dominant species present are not functionally diverse.

394 Functional dispersion, functional divergence, and Rao's quadratic entropy were all associated
395 with closed canopy habitats and thus may serve as more accurate indicators of forest recovery.
396 The observed increase in functional dispersion in mature forests could indicate higher degrees of
397 niche differentiation, where lower rates of competition in older sites may enhance species co-
398 occurrences and complementarity (O'Brien et al., 2022). Studies have suggested that
399 communities with higher functional dispersion may be better able to respond to environmental
400 changes (Flynn et al., 2011; Kuebbing et al., 2018). Similarly, the increase in functional
401 divergence in mature forests could suggest that the distribution of traits becomes more varied and

402 specialized in later stages of regeneration, allowing for greater resource partitioning and reduced
403 competition among species (Sayer et al., 2017).

404 Functional dispersion was driven by changes in both beak and wing length, whereas changes
405 in functional divergence were more strongly associated with in beak length. Longer beaks may
406 facilitate access to a wider range of food resources, including specialized foraging niches such as
407 probing into tree bark or nectar. Increased wing length in closed-canopy environments could
408 provide enhanced flight efficiency, enabling birds to navigate more complex environments.
409 Landscapes with higher tree cover facilitate the movement of species, where birds with larger
410 wings might have higher mobility across patches of degraded landscapes if the surrounding
411 forest has higher levels of canopy cover (Remeš et al., 2021). Furthermore, high Rao's quadratic
412 entropy values in mature forests signifies greater functional diversity overall, meaning the
413 species within a community have more distinct functional traits and are less functionally
414 redundant (Sayer et al., 2017). Changes in Rao's quadratic entropy were also driven by beak and
415 wing length and additionally included mass. Mass being associated with few functional diversity
416 indices indicates that body size influences resource use and habitat specialization independently
417 of other morphological traits. In structurally complex environments, larger-bodied species may
418 exploit different foraging strata or require larger territories, whereas smaller species may have
419 increased maneuverability in dense vegetation.

420 Other systems have also found contrasting patterns of taxonomic and functional diversity
421 indices in relation to forest regeneration. Some have found that regeneration time increases both
422 functional diversity and species diversity of bird communities (Ikin et al., 2019; Remeš et al.,
423 2021), however both studies only utilized one measure of functional or taxonomic diversity. Ikin
424 et al. (2019) found that species richness correlated with functional richness and, contrasting to

425 our findings, increased with forest cover. Another study observed an increase in functional
426 diversity as a function of forest regeneration in mammalian communities, however found no
427 differences in taxonomic diversity across regeneration stages (Derhé et al., 2018). In contrast,
428 others have found that regeneration did not significantly increase either functional or taxonomic
429 diversity (Barros et al., 2022). When focusing on individual functional diversity measures, one
430 study found that functional divergence, functional richness, and functional evenness of plant
431 communities changed independently of one another (Pakeman, 2011), similar to what we
432 observed in avian communities. These contrasting findings highlight the complexity of
433 biodiversity recovery, suggesting that taxonomic and functional diversity may respond
434 differently to forest regeneration depending on the taxa studied, the metrics used, and the specific
435 environmental conditions of the system.

436 The observed low rates of taxonomic diversity in closed-canopy forests could be due to low
437 detection rates from mist-net sampling. Therefore, substantial effort would be needed to saturate
438 a species accumulation curve and accurately account for a high proportion of the species residing
439 within these dense, biodiverse habitats. Since functional diversity indices were indicative of
440 closed-canopy habitat, these measures could potentially be a faster and more efficient way of
441 assessing community responses to forest regeneration as they require less sampling effort than
442 taxonomic assessments. However, not all functional diversity indices were characteristic of
443 regeneration, and some functional diversity indices are sensitive to under sampling (Kortmann et
444 al., 2025; Van Der Plas et al., 2017). It has been observed that functional evenness is highly
445 sensitive to under sampling, and functional richness is intermediately sensitive to under
446 sampling, making them potentially less useful in biodiversity surveys (Van Der Plas et al., 2017).
447 Functional divergence, function dispersion, and Rao's quadratic entropy were all less sensitive to

448 under sampling (Van Der Plas et al., 2017), and were strongly associated with closed-canopy
449 habitats might, making them more useful when aiming to understand the functional recovery of
450 communities across forest regeneration.

451 Despite its distinction between open and closed canopy habitats, functional diversity
452 measures did not elucidate differences between secondary and old-growth communities. This
453 could be due to the fact that we did not capture the full set of functional traits or environmental
454 gradients associated with changes in bird communities across regenerating forests. For example,
455 one study found that bird functional divergence increased with increasing variability in tree
456 diameter (Schuldt et al., 2022). Therefore, considering foraging behaviors such as cavity nesting,
457 bark gleaning, and sit-and-wait foraging might have explained the variation between secondary
458 and old growth habitats. However, another study found that avian functional dispersion and
459 functional divergence was comparable among secondary and old growth tropical forests (Sayer
460 et al., 2017), therefore this lack of differentiation between the two regeneration classes could be a
461 feature of closed-canopy forests. Future research should try to cover the scope of the drivers of
462 functional diversity bird community recovery, including varying environmental parameters and
463 behavioral traits.

464 Overall, our study contributes to the growing use of functional diversity indices as a means of
465 assessing biodiversity responses to forest regeneration. Our findings underscore the importance
466 of selecting robust functional diversity indices that are both ecologically meaningful and resilient
467 to sampling limitations when evaluating community responses to forest regeneration. By
468 prioritizing indices like functional divergence, functional dispersion, and Rao's quadratic
469 entropy, restoration practitioners can more reliably assess community functional recovery,
470 ultimately improving the effectiveness of biodiversity monitoring in regenerating forests.

471 **References**

- 472 Acevedo-Charry, O., & Aide, T. M. (2019). Recovery of amphibian, reptile, bird and mammal
473 diversity during secondary forest succession in the tropics. *Oikos*, *128*(8), 1065–1078.
474 <https://doi.org/10.1111/oik.06252>
- 475 Aguilar Mugica, S., Devenish, C., Wege, D. C., Anadón-Irizarry, V., & Balman, M. (2009).
476 *Important bird areas Americas: Priority sites for biodiversity conservation*. Birdlife
477 International.
- 478 Aguirre-Gutiérrez, J., WallisDeVries, M. F., Marshall, L., Zelfde, M., Villalobos-Arámbula, A.
479 R., Boekelo, B., Bartholomeus, H., Franzén, M., & Biesmeijer, J. C. (2017). Butterflies
480 show different functional and species diversity in relationship to vegetation structure
481 and land use. *Global Ecology and Biogeography*, *Oct*;26(10):1126-37.
- 482 Ausprey, I. J., Newell, F. L., & Robinson, S. K. (2022). Functional response traits and altered
483 ecological niches drive the disassembly of cloud forest bird communities in tropical
484 montane countrysides. *Journal of Animal Ecology*, *91*(11), 2314–2328.
485 <https://doi.org/10.1111/1365-2656.13816>
- 486 Barros, F. D. C., Almeida, S. M., Godoy, B. S., Silva, R. R. D., Silva, L. C., De Moraes, K. F., &
487 Santos, M. P. D. (2022). Taxonomic and functional diversity of bird communities in
488 mining areas undergoing passive and active restoration in eastern Amazon. *Ecological*
489 *Engineering*, *182*, 106721. <https://doi.org/10.1016/j.ecoleng.2022.106721>
- 490 Bello, C., Crowther, T. W., & Ramos, D. L. (2024). Frugivores enhance potential carbon
491 recovery in fragmented landscapes. *Nat. Clim. Chang*, *14*, 636–643.
- 492 Bodin, B., Garavaglia, V., Pingault, N., Ding, H., Wilson, S., Meybeck, A., Gitz, V., d’Andrea,
493 S., & Besacier, C. (2022). A standard framework for assessing the costs and benefits of
494 restoration: Introducing The Economics of Ecosystem Restoration. *Restoration Ecology*,
495 *30*(3), e13515. <https://doi.org/10.1111/rec.13515>
- 496 Cano-Barbacil, C., Radinger, J., Olden, J. D., & García-Berthou, E. (2023). Estimates of niche
497 position and breadth vary across spatial scales for native and alien inland fishes. *Global*
498 *Ecology and Biogeography*, *32*(3), 466–477. <https://doi.org/10.1111/geb.13630>
- 499 Carlo, T. A., & Morales, J. M. (2016). Generalist birds promote tropical forest regeneration and
500 increase plant diversity via rare-biased seed dispersal. *ECOLOGY*, *97*(7), 1819–1831.
501 <https://doi.org/10.1890/15-2147.1>
- 502 Chao, A., Gotelli, N. J., Hsieh, T. C., Sander, E. L., Ma, K. H., Colwell, R. K., & Ellison, A. M.
503 (2014). Rarefaction and extrapolation with Hill numbers: A framework for sampling
504 and estimation in species diversity studies. *Ecological Monographs*, *Feb*;84(1):45-67.
- 505 Chazdon, R. L. (2008). Beyond Deforestation: Restoring Forests and Ecosystem Services on
506 Degraded Lands. *Science*, *320*(5882), 1458–1460.
507 <https://doi.org/10.1126/science.1155365>
- 508 Chazdon, R. L. (2013). Making tropical succession and landscape reforestation successful.
509 *Journal of Sustainable Forestry*, *3*;32(7):649-58.

- 510 Chazdon, R. L., & Guariguata, M. R. (2016). Natural regeneration as a tool for large-scale forest
511 restoration in the tropics: Prospects and challenges. *Biotropica*, *v;48(6):716-30*.
- 512 Coddington, C. P. J., Cooper, W. J., Mokross, K., & Luther, D. A. (2023). Forest structure
513 predicts species richness and functional diversity in Amazonian mixed-species bird
514 flocks. *Biotropica*, *55(2)*, 467–479. <https://doi.org/10.1111/btp.13201>
- 515 Coops, N. C., Tompalski, P., Goodbody, T. R. H., Queinnec, M., Luther, J. E., Bolton, D. K.,
516 White, J. C., Wulder, M. A., Van Lier, O. R., & Hermosilla, T. (2021). Modelling lidar-
517 derived estimates of forest attributes over space and time: A review of approaches and
518 future trends. *Remote Sensing of Environment*, *260*, 112477.
519 <https://doi.org/10.1016/j.rse.2021.112477>
- 520 Crouzeilles, R., Curran, M., Ferreira, M. S., Lindenmayer, D. B., Grelle, C. E. V., & Rey
521 Benayas, J. M. (2016). A global meta-analysis on the ecological drivers of forest
522 restoration success. *Nature Communications*, *7(1)*, 11666.
523 <https://doi.org/10.1038/ncomms11666>
- 524 Derhé, M. A., Murphy, H. T., Preece, N. D., Lawes, M. J., & Menéndez, R. (2018). Recovery of
525 mammal diversity in tropical forests: A functional approach to measuring restoration.
526 *Restoration Ecology*.
- 527 Durães, R., Carrasco, L., Smith, T. B., & Karubian, J. (2013). Effects of forest disturbance and
528 habitat loss on avian communities in a Neotropical biodiversity hotspot. *Biological*
529 *Conservation*, *166*, 203–211. <https://doi.org/10.1016/j.biocon.2013.07.007>
- 530 Ellison, A. M. (2010). Partitioning diversity. *Ecology*, *1;91(7):1962-3*.
- 531 Flynn, D. F. B., Mirotnick, N., Jain, M., Palmer, M. I., & Naeem, S. (2011). Functional and
532 phylogenetic diversity as predictors of biodiversity–ecosystem–function relationships.
533 *Ecology*, *92(8)*, 1573–1581. <https://doi.org/10.1890/10-1245.1>
- 534 Freile, J. F., & Restall, R. L. (2018). *Birds of Ecuador*. Helm, Bloomsbury Publishing Plc.
- 535 Gao, J., Yan, D., Ndithia, H. K., Imboma, T., Mutati, A. S., Kioko, O., Gichuki, P., Wu, F.,
536 Kioko, E. N., & Yang, X. (2024). Patterns and mechanisms of bird community
537 assembly along an Afrotropical elevational gradient in Kenya. *Global Ecology and*
538 *Conservation*, *53*, e02997. <https://doi.org/10.1016/j.gecco.2024.e02997>
- 539 Gregory, R. D., & Gaston, K. J. (2000). Explanations of commonness and rarity in British
540 breeding birds: Separating resource use and resource availability. *Oikos*, *88(3)*, 515–
541 526. <https://doi.org/10.1034/j.1600-0706.2000.880307.x>
- 542 Helms, J. A., Woerner, C. R., Fawzi, N. I., MacDonald, A., Juliansyah, Pohnan, E., & Webb, K.
543 (2018). Rapid Response of Bird Communities to Small-Scale Reforestation in
544 Indonesian Borneo. *Tropical Conservation Science*, *11*, 194008291876946.
545 <https://doi.org/10.1177/1940082918769460>
- 546 Holl, K. D. (1999). Factors Limiting Tropical Rain Forest Regeneration in Abandoned Pasture:
547 Seed Rain, Seed Germination, Microclimate, and Soil†. *Biotropica*, *31*, 229–242.
548 <https://doi.org/10.1111/j.1744-7429.1999.tb00135.x>

- 549 Howe, H. F., & Smallwood, J. (1982). Ecology of Seed Dispersal. *Annual Review of Ecology*
550 *and Systematics*, 13(1), 201–228. <https://doi.org/10.1146/annurev.es.13.110182.001221>
- 551 Ikin, K., Barton, P. S., Blanchard, W., Crane, M., Stein, J., & Lindenmayer, D. B. (2019). Avian
552 functional responses to landscape recovery. *Proceedings of the Royal Society B*. 2019
553 *Apr*, 286(20190114).
- 554 Karadimou, E. K., Kallimanis, A. S., Tsiripidis, I., & Dimopoulos, P. (2016). Functional
555 diversity exhibits a diverse relationship with area, even a decreasing one. *Scientific*
556 *Reports*, 6(1), 35420. <https://doi.org/10.1038/srep35420>
- 557 Kleemann, J., Zamora, C., Villacis-Chiluisa, A. B., Cuenca, P., Koo, H., Noh, J. K., Fürst, C., &
558 Thiel, M. (2022). Deforestation in Continental Ecuador with a Focus on Protected
559 Areas. *Land*, 11(2), 268. <https://doi.org/10.3390/land11020268>
- 560 Kormann, U., Scherber, C., Tschamtker, T., Klein, N., Larbig, M., Valente, J. J., Hadley, A. S., &
561 Betts, M. G. (2016). Corridors restore animal-mediated pollination in fragmented
562 tropical forest landscapes. *Proceedings of the Royal Society B: Biological Sciences*,
563 283(1823), 20152347. <https://doi.org/10.1098/rspb.2015.2347>
- 564 Kortmann, M., Chao, A., Schaefer, H. M., Blüthgen, N., Gelis, R., Tremlett, C. J., Busse, A.,
565 Püls, M., Seibold, S., Kriegel, P., Rabl, D., De La Hoz, M., Şekercioğlu, Ç. H.,
566 Schleuning, M., Feldhaar, H., Newell, F. L., Kümmer, S., Mitesser, O., Peters, M. K., &
567 Müller, J. (2025). Sample coverage affects diversity measures of bird communities
568 along a natural recovery gradient of abandoned agriculture in tropical lowland forests.
569 *Journal of Applied Ecology*, 1365-2664.14879. [https://doi.org/10.1111/1365-](https://doi.org/10.1111/1365-2664.14879)
570 [2664.14879](https://doi.org/10.1111/1365-2664.14879)
- 571 Kuebbing, S. E., Maynard, D. S., & Bradford, M. A. (2018). Linking functional diversity and
572 ecosystem processes: A framework for using functional diversity metrics to predict the
573 ecosystem impact of functionally unique species. *Journal of Ecology*, 106(2), 687–698.
574 <https://doi.org/10.1111/1365-2745.12835>
- 575 Laliberté, E., Legendre, P., & Shipley, B. (2014). *FD: measuring functional diversity from*
576 *multiple traits, and other tools for functional ecology*.
- 577 Lamb, D. (2018). Undertaking large-scale forest restoration to generate ecosystem services.
578 *Restoration Ecology*, 26(4), 657–666. <https://doi.org/10.1111/rec.12706>
- 579 Latja, P., Valtonen, A., Malinga, G. M., & Roininen, H. (2016). Active restoration facilitates bird
580 community recovery in an Afrotropical rainforest. *Biological Conservation*, 200, 70–79.
581 <https://doi.org/10.1016/j.biocon.2016.05.035>
- 582 Lee, A. T. (2018). Why Birds Matter: Avian Ecological Function and Ecosystem Services.
583 *Ostrich*, 89(2), 203–204. <https://doi.org/10.2989/00306525.2018.1465788>
- 584 Legendre, P., & Gallagher, E. D. (2001). Ecologically meaningful transformations for ordination
585 of species data. *Oecologia*.
- 586 Maire, E., Grenouillet, G., Brosse, S., & Villéger, S. (2015). How Many Dimensions Are Needed
587 to Accurately Assess Functional Diversity? A Pragmatic Approach for Assessing the

588 Quality of Functional Spaces. *Global Ecology and Biogeography*, 24(6), 728–740.
589 <https://doi.org/10.1111/geb.12299>.

590 Malhi, Y., Riutta, T., Wearn, O. R., Deere, N. J., Mitchell, S. L., Bernard, H., Majalap, N., Nilus,
591 R., Davies, Z. G., Ewers, R. M., & Struebig, M. J. (2022). Logged tropical forests have
592 amplified and diverse ecosystem energetics. *Nature*, 612(7941), 707–713.
593 <https://doi.org/10.1038/s41586-022-05523-1>

594 Modiba, R. V., Joseph, G. S., Seymour, C. L., Fouché, P., & Foord, S. H. (2017). Restoration of
595 riparian systems through clearing of invasive plant species improves functional diversity
596 of Odonate assemblages. *Biological Conservation*, 214, 46–54.

597 Moreno-Mateos, D., Alberdi, A., Morriën, E., van der Putten, W. H., Rodríguez-Uña, A., &
598 Montoya, D. (2020). The long-term restoration of ecosystem complexity. *Nature
599 Ecology & Evolution*, 4(5), 676–685. <https://doi.org/10.1038/s41559-020-1154-1>

600 Morrison, E. B., & Lindell, C. A. (2012). Birds and bats reduce insect biomass and leaf damage
601 in tropical forest restoration sites. *Ecological Applications*, 22(5), 1526–1534.
602 <https://doi.org/10.1890/11-1118.1>

603 Nabhan, G. P., Orlando, L., Smith Monti, L., & Aronson, J. (2020). Hands-On Ecological
604 Restoration as a Nature-Based Health Intervention: Reciprocal Restoration for People
605 and Ecosystems. *Ecopsychology*, 12(3), 195–202.
606 <https://doi.org/10.1089/eco.2020.0003>

607 O'Brien, S. A., Dehling, D. M., & Tylianakis, J. M. (2022). The recovery of functional diversity
608 with restoration. *Ecology*, 103(3), e3618. <https://doi.org/10.1002/ecy.3618>

609 Oksanen, J., Simpson, G., Blanchet, F., Kindt, R., Legendre, P., Minchin, P., O'hara, R.,
610 Solymos, P., Stevens, M., & Szoecs, E. (2022). *Wagner H. vegan: Community Ecology
611 Package. R package version* (p. 2 6-4).

612 Oliveira, B. F., & Scheffers, B. R. (2019). Vertical stratification influences global patterns of
613 biodiversity. *Ecography*, Feb;42(2):249.

614 Owen, K. C., Melin, A. D., Campos, F. A., Fedigan, L. M., Gillespie, T. W., & Mennill, D. J.
615 (2020). Bioacoustic analyses reveal that bird communities recover with forest
616 succession in tropical dry forests. *Avian Conservation and Ecology*, 15(1), art25.
617 <https://doi.org/10.5751/ACE-01615-150125>

618 Pakeman, R. J. (2011). Functional diversity indices reveal the impacts of land use intensification
619 on plant community assembly: Drivers of functional diversity. *Journal of Ecology*,
620 99(5), 1143–1151. <https://doi.org/10.1111/j.1365-2745.2011.01853.x>

621 Pena, R., Schleuning, M., Dalerum, F., Donoso, I., Rodriguez-Perez, J., & Garcia, D. (2023).
622 Abundance and trait-matching both shape interaction frequencies between plants and
623 birds in seed-dispersal networks. *BASIC AND APPLIED ECOLOGY*, 66, 11–21.
624 <https://doi.org/10.1016/j.baae.2022.11.008>

625 Pinotti, B. T., Pagotto, C. P., & Pardini, R. (2012). Habitat structure and food resources for
626 wildlife across successional stages in a tropical forest. *Forest Ecology and
627 Management*, 283, 119–127. <https://doi.org/10.1016/j.foreco.2012.07.020>

- 628 Podani, J. (1999). Extending Gower's general coefficient of similarity to ordinal characters.
629 *Taxon*.
- 630 Quitian, M., Santillan, V., Bender, I. M. A., Ivan Espinosa, C., Homeier, J., Boehning-Gaese, K.,
631 Schleuning, M., & Neuschulz, E. L. (2019). Functional responses of avian frugivores to
632 variation in fruit resources between natural and fragmented forests. *FUNCTIONAL*
633 *ECOLOGY*, 33(3), 399–410. <https://doi.org/10.1111/1365-2435.13255>
- 634 Reid, J. L., Harris, J. B. C., & Zahawi, R. A. (2012). Avian Habitat Preference in Tropical Forest
635 Restoration in Southern Costa Rica. *Biotropica*, 44(3), 350–359.
636 <https://doi.org/10.1111/j.1744-7429.2011.00814.x>
- 637 Remeš, V., Remešová, E., Friedman, N. R., Matysioková, B., & Rubáčová, L. (2021). Functional
638 diversity of avian communities increases with canopy height: From individual behavior
639 to continental-scale patterns. *Ecology and Evolution*, Sep; 11(17): 11839-51.
- 640 Sayer, C. A., Bullock, J. M., & Martin, P. A. (2017). Dynamics of avian species and functional
641 diversity in secondary tropical forests. *Biological Conservation*, 211, 1–9.
642 <https://doi.org/10.1016/j.biocon.2017.05.004>
- 643 Schuldt, A., Huke, P., Glatthorn, J., Hagge, J., Wildermuth, B., & Matevski, D. (2022). Tree
644 mixtures mediate negative effects of introduced tree species on bird taxonomic and
645 functional diversity. *Journal of Applied Ecology*, 59(12), 3049–3060.
646 <https://doi.org/10.1111/1365-2664.14300>
- 647 Segurado, D., and Silman, M. (2023). Restauracion Processing Report. Unpublished data.
648 Accessed August 2023.
- 649 Team, R. C. (2022). *R: A Language and Environment for Statistical Computing*. R Foundation
650 for Statistical Computing, Vienna. <https://www.R-project.org>
- 651 Tobias, J. A., Sheard, C., Pigot, A. L., Devenish, A. J. M., Yang, J., Sayol, F., Neate-Clegg, M.
652 H. C., Alioravainen, N., Weeks, T. L., Barber, R. A., Walkden, P. A., MacGregor, H. E.
653 A., Jones, S. E. I., Vincent, C., Phillips, A. G., Marples, N. M., Montaña-Centellas, F.
654 A., Leandro-Silva, V., Claramunt, S., ... Schleuning, M. (2022). AVONET:
655 Morphological, ecological and geographical data for all birds. *Ecology Letters*, 25(3),
656 581–597. <https://doi.org/10.1111/ele.13898>
- 657 Van Der Hoek, Y. (2017). The potential of protected areas to halt deforestation in Ecuador.
658 *Environmental Conservation*, 44(2), 124–130.
659 <https://doi.org/10.1017/S037689291700011X>
- 660 Van Der Plas, F., Van Klink, R., Manning, P., Olf, H., & Fischer, M. (2017). Sensitivity of
661 functional diversity metrics to sampling intensity. *Methods in Ecology and Evolution*,
662 8(9), 1072–1080. <https://doi.org/10.1111/2041-210X.12728>
- 663 Viana-Soto, A., García, M., Aguado, I., & Salas, J. (2022). Assessing post-fire forest structure
664 recovery by combining LiDAR data and Landsat time series in Mediterranean pine
665 forests. *International Journal of Applied Earth Observation and Geoinformation*, 108,
666 102754. <https://doi.org/10.1016/j.jag.2022.102754>

- 667 Villéger, S., Mason, N. W., & Mouillot, D. (2008). New multidimensional functional diversity
668 indices for a multifaceted framework in functional ecology. *Ecology*, *Aug;89(8):2290-*
669 *301*.
- 670 Wickham, H., Chang, W., & Wickham, M. H. (2016). Package ‘ggplot2’. Create elegant data
671 visualisations using the grammar of graphics. *Version*, *2(1)*, 1–89.
- 672 Williams, B. A., Beyer, H. L., Fagan, M. E., Chazdon, R. L., Schmoeller, M., Sprenkle-
673 Hyppolite, S., Griscom, B. W., Watson, J. E. M., Tedesco, A. M., Gonzalez-Roglich,
674 M., Daldegan, G. A., Bodin, B., Celentano, D., Wilson, S. J., Rhodes, J. R., Alexandre,
675 N. S., Kim, D.-H., Bastos, D., & Crouzeilles, R. (2024). Global potential for natural
676 regeneration in deforested tropical regions. *Nature*, *636(8041)*, 131–137.
677 <https://doi.org/10.1038/s41586-024-08106-4>
- 678 Wunderle, J. M. (1997). The role of animal seed dispersal in accelerating native forest
679 regeneration on degraded tropical lands. *Forest Ecology and Management*, *99(1–2)*,
680 *223–235*. [https://doi.org/10.1016/S0378-1127\(97\)00208-9](https://doi.org/10.1016/S0378-1127(97)00208-9)
- 681 Zahawi, R. A., Dandois, J. P., Holl, K. D., Nadwodny, D., Reid, J. L., & Ellis, E. C. (2015).
682 Using lightweight unmanned aerial vehicles to monitor tropical forest recovery.
683 *Biological Conservation*, *186*, 287–295. <https://doi.org/10.1016/j.biocon.2015.03.031>
684

Supplementary Table 1: Description of each functional trait obtained for each bird species, including its variable type, measurement metric, and functional importance.

Trait	Variable	Description	Functional Importance
Beak Length (mm)	Continuous	Length from the tip of the beak to the base of the skull	Refers to different feeding strategies relating to functional role of species (e.g., seed-dispersers, pollinators).
Beak Width (mm)	Continuous	Width of the beak at the anterior edge of the nostrils	Refers to different feeding strategies relating to functional role of species (e.g., seed-dispersers, pollinators).
Wing Length (mm)	Continuous	Length from the carpal joint (bend of the wing) to the tip of the longest primary feather on the flattened wing	Flight performance, migration, feeding ability. Birds with shorter wings are typically suited for denser vegetation, while birds with larger wings can cover more range and aid in habitat connectivity.
Mass (g)	Continuous	Body mass given as species average (incorporating both male and female body mass)	Energy requirements, activity levels, environmental conditions. Larger-bodied birds require more food to maintain energy and, thus, may play important environmental roles such as dispersing large seeds across landscapes.
Primary Habitat	Categorical	Primary habitat species are found in, including human-modified, shrubland, and forests	Refers to species' ability to perform functional roles across multiple landscapes. Species adapted to human-modified landscapes may be important in connecting disturbed areas to non-disturbed areas.
Trophic Niche/Diet Type	Categorical	Species are put into certain categories if over 60% of their diet is made up of one food source (e.g., frugivore, nectarivore)	Refers to different feeding strategies relating to the functional role of species (e.g., seed-dispersers, pollinators).

Supplementary Table 2: Bird community data for species surveyed across the entire FCAT Reserve. Species codes represent 4-digit codes based on each species' common name. Trait data, including trophic niches, habitat associations, and morphological traits for each species were collected using an open access data set provided by Tobias et al., 2022. Morphological traits include average mass (g), beak length (mm), beak width (mm), wing length (mm), and tail length (mm). Abundance represents the total number of individuals observed during the study.

Cod e	Scientific Name	Trophic Niche	Habitat	A b u n d a n c e	M a s s	B e a k L e n g t h	B e a k W i d t h	W i n g L e n g t h	T a i l L e n g t h
AMHB	<i>Amazilia amazilia</i>	Nectarivore	Shrubland	2	4.3	20.7	2.9	61.8	37.6
BABW	<i>Campylorhynchus zonatus</i>	Invertivore	Forest	1	34.6	24	3.9	78.4	82
BANA	<i>Coereba flaveola</i>	Nectarivore	Shrubland	24	10	13.2	3.6	54.6	34.1
BAWS	<i>Pygochelidon cyanoleuca</i>	Invertivore	Human Modified	1	9.7	8.6	3.6	92.3	48.8
BAYW	<i>Cantorchilus nigricapillus</i>	Invertivore	Forest	4	23.9	19.2	4.2	65.8	54.3
BBSC	<i>Campylorhamphus pusillus</i>	Invertivore	Forest	1	40.5	55	4.2	95.6	95
BCAS	<i>Thamnophilus atrinucha</i>	Invertivore	Forest	5	23.6	19.4	5.4	67.9	56.1
BCHH	<i>Amazilia amabilis</i>	Nectarivore	Forest	20	4.3	21.3	2	52.3	29.2
BCOF	<i>Myiophobus fasciatus</i>	Invertivore	Shrubland	7	9.9	13.5	5	58.9	54.1
BCRM	<i>Lepidothrix coronata</i>	Frugivore	Forest	16	8.3	10.9	3.7	56.8	26.6
BFDA	<i>Dacnis lineata</i>	Frugivore	Forest	2	11	13	3.5	58	40.6
BGRA	<i>Volatinia jacarina</i>	Granivore	Human Modified	4	9.9	10.4	4.3	47.8	42.8
BGRO	<i>Cyanoloxia cyanoides</i>	Granivore	Forest	3	32.5	19.6	10.2	79.6	66.8
BGTA	<i>Tangara episcopus</i>	Omnivore	Forest	7	35	14.2	6.4	87.3	64
BHTA	<i>Tangara gyrola</i>	Frugivore	Forest	2	21	12.7	4.8	73.5	51.4

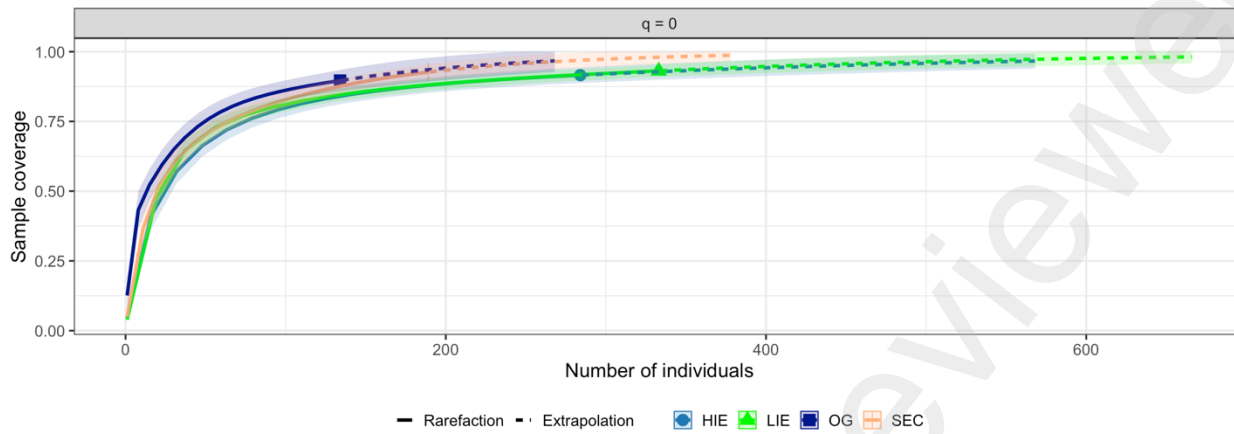
BIAN	<i>Gymnopithys bicolor</i>	Invertivore	Forest	7	31.1	18.5	5.1	75.3	46.6
BNTA	<i>Tangara cyanicollis</i>	Frugivore	Forest	9	17	12.3	4.5	66.1	46.5
BRAT	<i>Attila spadiceus</i>	Invertivore	Forest	2	39.1	22.3	7.3	85.6	67.8
BTBA	<i>Threnetes ruckeri</i>	Nectarivore	Forest	34	5.2	33.4	3	56.6	36.3
BTFG	<i>Automolus ochrolaemus</i>	Invertivore	Forest	2	40.2	22.7	4.8	87.1	74.8
BTSA	<i>Saltator maximus</i>	Frugivore	Shrubland	8	47.6	20.7	8.9	96.1	88.9
BURW	<i>Myiothlypis fulvicauda</i>	Invertivore	Forest	6	14.9	14.3	4.5	63.3	49.7
CBAN	<i>Poliocrania exsul</i>	Invertivore	Forest	4	26.5	21.1	5	66.6	47.3
CHTY	<i>Zimmerius albigularis</i>	Invertivore	Forest	16	10.4	9	3.2	49.6	44.5
CHWA	<i>Myiothlypis chlorophrys</i>	Invertivore	Forest	3	16.2	12.9	4.6	61	48.1
CIMB	<i>Pachyramphus cinnamomeus</i>	Invertivore	Forest	3	20.3	16.8	7.6	77	59.4
CIVI	<i>Vireo chivi</i>	Invertivore	Forest	14	16.1	14	4.4	68	52.1
COAR	<i>Pteroglossus torquatus</i>	Frugivore	Forest	2	219.1	104	22.9	146.9	150.5
COTF	<i>Todirostrum cinereum</i>	Invertivore	Shrubland	10	6.3	14.8	4.8	42.5	33.8
CRWO	<i>Thalurania colombica</i>	Nectarivore	Forest	12	4.5	20.4	2.3	52.3	33.1
CTST	<i>Epinecrophylla fulviventris</i>	Invertivore	Forest	6	10.4	15	4.1	50.9	33.2
DCGQ	<i>Asemospiza obscura</i>	Granivore	Shrubland	64	11.2	10.4	4.8	52.4	42.3
DUAN	<i>Cercomacroides tyrannina</i>	Invertivore	Forest	1	16.3	18.2	4.9	62.7	60.4
DUPI	<i>Patagioenas goodsoni</i>	Frugivore	Forest	1	176	17	4	148.7	99.6
DWAN	<i>Microrhopias quixensis</i>	Invertivore	Forest	2	7.9	15.6	4.1	53	52.7
ECTR	<i>Turdus maculirostris</i>	Omnivore	Forest	4	69.6	22.5	4.9	112.6	97.7
FRTA	<i>Ramphocelus flammigerus</i>	Frugivore	Forest	15	33	18.4	8.2	88.6	74.8
GAGW	<i>Myiothlypis fraseri</i>	Invertivore	Woodland	1	11.6	13.5	5	65	55.7
GANT	<i>Taraba major</i>	Invertivore	Forest	1	59.2	26.3	7	90.6	81
GBAN	<i>Crotophaga sulcirostris</i>	Invertivore	Human Modified	1	82	26.9	9.5	129.3	162.7
GCBR	<i>Heliodoxa jacula</i>	Nectarivore	Forest	5	8.1	26.4	2.5	70.3	44.2
GMAK	<i>Cryptopipo litae</i>	Frugivore	Forest	8	14.9	13.3	4.3	69.2	46.8
GOWO	<i>Colaptes rubiginosus</i>	Invertivore	Forest	1	55.8	27	7.1	123.7	76.3
GRET	<i>Discosura conversii</i>	Nectarivore	Forest	3	3	14.4	1.3	42.2	42
GRHO	<i>Chlorophanes spiza</i>	Frugivore	Forest	6	19	15.9	4.5	68.3	48.2
GYBM	<i>Progne chalybea</i>	Invertivore	Shrubland	1	50	15.3	5.6	130.6	66.4

HOWR	<i>Troglodytes aedon</i>	Invertivore	Shrubland	19	10.9	15.9	3	51.4	41.1
LBST	<i>Heliomaster longirostris</i>	Nectarivore	Forest	1	6.6	35	2.7	58.4	30.7
MUTO	<i>Ciccaba virgata</i>	Omnivore	Forest	1	284	33	9	240.6	149.1
NOSC	<i>Schiffornis veraepacis</i>	Omnivore	Forest	6	31.1	21.2	5.3	87.3	70.2
OBEE	<i>Euphonia xanthogaster</i>	Frugivore	Forest	22	13	10.7	4.8	61.4	36
OBFL	<i>Mionectes oleagineus</i>	Frugivore	Forest	21	11.2	11.8	4.2	60.5	48.2
OBSP	<i>Arremon aurantirostris</i>	Omnivore	Forest	4	34.5	16	6.6	72.7	66.4
OCEE	<i>Euphonia saturata</i>	Frugivore	Forest	2	13.3	10	3.9	57.7	32.3
OCYE	<i>Geothlypis semiflava</i>	Invertivore	Shrubland	4	17.2	14.7	3.3	59.7	52.7
ORFC	<i>Myiopiccus ornatus</i>	Invertivore	Forest	2	10.6	10.3	3.6	52.4	26.5
OLPI	<i>Picumnus olivaceus</i>	Invertivore	Forest	5	10.6	10.3	3.6	52.4	26.5
OLWO	<i>Sittasomus griseicapillus</i>	Invertivore	Forest	4	13.1	16.1	4	76.7	76.5
ORFL	<i>Myiopiccus ornatus</i>	Invertivore	Forest	5	9.9	13.2	5.4	59.6	41.2
OSFT	<i>Mionectes olivaceus</i>	Frugivore	Forest	26	15.3	13.7	4.1	69	40
PAAN	<i>Myrmotherula pacifica</i>	Invertivore	Shrubland	6	10.1	15.3	3.6	50.6	28
PAPA	<i>Forpus coelestis</i>	Omnivore	Shrubland	1	26.1	16.6	9.4	76.8	39.4
PATA	<i>Tangara palmarum</i>	Omnivore	Forest	1	39	15	5.9	92.5	70.4
PBRW	<i>Dendrocicla fuliginosa</i>	Invertivore	Forest	5	38.7	29.9	6.4	104.9	86.7
PCFA	<i>Heliodytes barroti</i>	Nectarivore	Forest	3	5.5	21.9	2.2	63.8	57
PCHU	<i>Amazilia rosenbergi</i>	Nectarivore	Forest	4	3.7	23.9	2.2	52.8	30
PLXE	<i>Xenops minutus</i>	Invertivore	Forest	2	10.6	13.1	2.8	55.7	43.6
PVTH	<i>Turdus obsoletus</i>	Omnivore	Forest	2	74.8	22.2	5	116	86.1
RCMA	<i>Ceratopipra mentalis</i>	Frugivore	Forest	15	15	12.1	4.4	58.5	28
RFSP	<i>Cranioleuca erythrogastra</i>	Invertivore	Forest	1	16.9	14.6	3.2	64.8	71.4
RMFL	<i>Myiozetetes cayanensis</i>	Invertivore	Shrubland	1	25.9	14.4	5.4	84.1	71.4
RTAH	<i>Amazilia tzacatl</i>	Nectarivore	Forest	22	4.8	21.9	3.1	56.4	34.2
RUFP	<i>Lipaugus unirufus</i>	Frugivore	Forest	1	82.1	24	7.2	132.4	112
SBAN	<i>Crotophaga ani</i>	Omnivore	Human Modified	2	110.1	30.6	9.9	144	180.6
SCBW	<i>Microcerculus marginatus</i>	Invertivore	Forest	2	18.2	19.2	3.4	58.7	24.2
SCFC	<i>Myiarchus phaeocephalus</i>	Invertivore	Woodland	1	26.3	22.5	7.1	93	89.8
SCPT	<i>Lophotriccus pileatus</i>	Invertivore	Forest	2	7.5	13.2	3.6	48.9	39.3

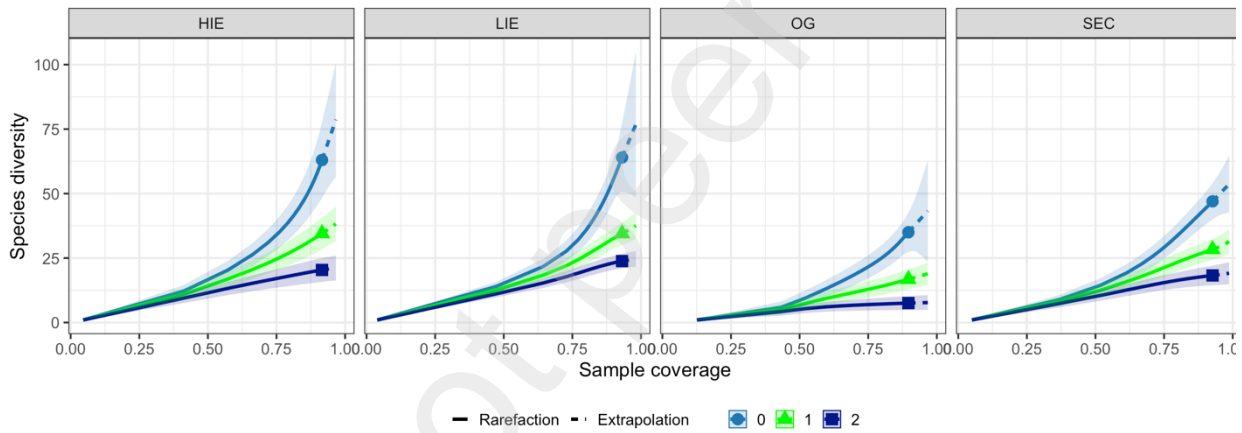
SHTY	<i>Phyllomyias griseiceps</i>	Invertivore	Forest	1	7.2	9	3.7	51.6	45.2
SHWO	<i>Lepidocolaptes souleyetii</i>	Invertivore	Woodland	3	25.7	32.7	4.1	92.3	84.5
SLAN	<i>Myrmotherula schisticolor</i>	Invertivore	Forest	3	9.6	15.5	3.3	54.9	36.9
SLSP	<i>Synallaxis brachyura</i>	Invertivore	Shrubland	28	18.3	16.3	3.4	57.9	76.7
SOBT	<i>Camptostoma obsoletum</i>	Invertivore	Shrubland	5	8.1	9.8	3.2	52.3	40.9
SPWO	<i>Xiphorhynchus erythropygius</i>	Invertivore	Forest	3	46.8	34.8	5.4	115.6	108.1
SQCU	<i>Piaya cayana</i>	Invertivore	Forest	1	102	32	8.8	145.5	278.6
SRFL	<i>Myiobius sulphureipygius</i>	Invertivore	Forest	6	11.6	14.6	4.2	66.4	56.2
SRWS	<i>Stelgidopteryx serripennis</i>	Invertivore	Shrubland	3	15.7	10.5	3.4	107.5	47.8
STFL	<i>Mionectes olivaceus</i>	Frugivore	Forest	2	15.3	13.7	4.1	69	40
STHR	<i>Phaethornis striigularis</i>	Nectarivore	Forest	6	3	23.7	2.4	39.1	36.4
STTA	<i>Tangara icterocephala</i>	Frugivore	Forest	4	22	12.6	5.1	70.5	45
STXE	<i>Xenops rutilus</i>	Invertivore	Forest	1	11.2	13.3	2.9	65.8	49
TBEU	<i>Euphonia lanirostris</i>	Frugivore	Forest	28	15	10.1	5.6	61	37.1
TBSF	<i>Sporophila funerea</i>	Granivore	Human Modified	48	13	12.6	6.9	55	48.7
TCTA	<i>Chrysocorypha delatrii</i>	Invertivore	Forest	1	18	15.2	4.9	71.4	58.1
VASE	<i>Sporophila corvina</i>	Granivore	Human Modified	40	10.6	10.7	5.3	52.9	42.8
VBHU	<i>Amazilia julie</i>	Nectarivore	Forest	14	3.3	16	1.2	43.1	26
WBM A	<i>Manacus manacus</i>	Frugivore	Forest	26	16.7	11.5	4.4	52.2	32.8
WBW O	<i>Glyphorhynchus spirurus</i>	Invertivore	Forest	3	14.6	13.7	4.4	68.7	66
WFLA	<i>Myrmotherula axillaris</i>	Invertivore	Forest	3	8.1	15	3.4	50.9	36.5
WSTA	<i>Tachyphonus rufus</i>	Invertivore	Shrubland	1	34.4	18.7	6.1	83	77.2
WTGS	<i>Atticora tibialis</i>	Invertivore	Forest	1	10.6	7.4	3.4	88.2	53
WTRS	<i>Platyrinchus mystaceus</i>	Invertivore	Forest	4	9.7	13.1	7.3	55	29.9
WTSI	<i>Eutoxeres aquila</i>	Nectarivore	Forest	13	10.6	27.5	3.6	70.5	54
WWH E	<i>Phaethornis yaruqui</i>	Nectarivore	Forest	98	5.4	45.6	2.6	59.5	53.8
WWPU	<i>Malacoptila panamensis</i>	Invertivore	Forest	6	42.6	29.3	9.5	87.4	71.8
YBEL	<i>Elaenia flavogaster</i>	Invertivore	Woodland	3	24.8	12.7	5	77.4	70.6
YBSE	<i>Sporophila nigricollis</i>	Granivore	Shrubland	35	9.6	9.1	5	52.4	43

YBSI	<i>Spinus xanthogastrus</i>	Granivore	Forest	2	12.7	10.5	4.3	65.2	40.5
YCTY	<i>Tyrannulus elatus</i>	Invertivore	Shrubland	3	7	8.3	3.2	48.2	40.7
YOFL	<i>Tolmomyias sulphurescens</i>	Invertivore	Forest	1	14.3	13.4	5.4	63	55.5

A)



B)



Supplementary Figure 1: Sampling completeness curves across four habitat types, representing different stages of regeneration and old-growth forest. The curves are color-coded: blue for HIE plots, green for LIE plots, pink for SEC plots, and purple for OG plots. A) Displays the overall sample coverage between sites where all plots within each habitat type are aggregated together, while B) examines the hill numbers/species diversity within each plot, where $q = 0$ (species richness), $q = 1$ (Shannon Diversity), and $q = 2$ (inverse Simpson).

Preprint not peer reviewed

Supplementary Table 3: Type II Wald chi-square tests assessing diversity indices as a function of regeneration stage (HIE, LIE, SEC, OG). Generalized least squares (GLS) regression was used to account for spatial dependence in model residuals, with a Gaussian spatial correlation structure applied. Significant relationships ($p < 0.05$) are highlighted in bold.

Response Variable	Chi Squared	P- Value
Species Richness (Q0)	34.44	< 0.001
Shannon Entropy (Q1)	79.32	< 0.001
Inverse Simpson Index (Q2)	25.66	< 0.001
Functional Richness (FRic)	11.46	0.001
Functional Divergence (FDiv)	14.27	0.002
Functional Evenness (FEve)	4.42	0.22
Functional Dispersion (FDis)	35.60	< 0.001
Rao's Quadratic Entropy (RaoQ)	20.98	< 0.001

690

691